

Remarks

This paper is being filed in response to the Office Action mailed on February 8, 2005. Per the petition and fee submitted herewith, the Applicants extend the period for filing this paper by three months from May 8, 2005 to August 8, 2005. Please charge any further fee that may be due, or credit any overpayment, to deposit account no. 50-2719. This paper is being filed along with a Request for Continued Examination under 37 C.F.R. 1.114. In view of the remarks presented below, the Applicants request reconsideration of the claims.

Claims 9-15 are pending in the application, and have been rejected under 35 U.S.C. 101 as allegedly lacking utility.

The Applicants acknowledge the withdrawal of the rejection under 35 U.S.C. 102.

The Applicants also note with appreciation that the Examiner recognizes the teaching of specification and art of record for (1) what the TASK protein is, and (2) how it functions, and that the utilities asserted in the specification are therefore credible. Nevertheless, the Office Action still indicates that the specification and art of record collectively fail to teach (3) a specific and substantial utility for the claimed TASK proteins. In particular, the Office Action alleges that the specification does not teach a “well established utility,” corresponding to a specific and substantial utility which is well known, immediately apparent, or implied by the specification’s disclosure of the properties of TASK protein, either alone or taken with the knowledge of one skilled in the art. The Applicants respectfully disagree.

As discussed in the Response filed on November 9, 2004, the Applicants’ specification sets forth several utilities for the claimed TASK proteins. Where one or more uses for an invention are disclosed in the specification, a rejection for lack of utility should not be made or maintained unless there is reason to doubt the objective truth of the asserted utility. Such a reason may be established when the written description suggests an inherently unbelievable undertaking or involves implausible scientific principles. *In re Cortright*, 49 USPQ2d 1464, 1466 (Fed. Cir. 1999). Further, a claimed invention need not accomplish every asserted utility. As long as the claimed invention meets at least on stated utility, the utility requirement is satisfied. *Stifung v. Renishaw PLC*, 20USPQ2d 1094, 1100 (Fed. Cir. 1991). Here, the Applicants’ specification does **not** suggest that the asserted utilities for the claimed TASK

proteins involves an inherently unbelievable undertaking or implausible scientific principles. On the contrary, as the Examiner notes in the Office Action, these asserted utilities are credible.

The Office Action states on pg. 3 that “the utilities asserted for the claimed TASK proteins are applicable to a general class of proteins, and have not been correlated to specific modulation of any particular event for a specific purpose.” This is not correct.

As discussed in paragraph [0069], the specification teaches that TASK is expressed in many different tissues, and notably in neurons like granular cells of the cerebellum. In these cells, TASK behaves like a K^+ -selective hole, which is extremely sensitive to extracellular pH in the physiological range between 6.5 and 7.8. *See, e.g.*, paragraph [0084]. The specification also teaches that the physiological function of the TASK channel is associated with modulation by external protons, which is observed in physiopathological situations such as epileptiform activity and spreading depression. *See, e.g.*, paragraph [0085].

Thus, the specification concludes that screening procedures for identifying substances that modulate TASK activity make it possible to identify drugs that may be useful in the treatment of diseases of the heart or of the nervous system; for example, epilepsy, heart (arrhythmias) and vascular diseases, neurodegenerative diseases, especially those associated with ischemia or anoxia, the endocrine diseases associated with anomalies of hormone secretion, muscle diseases. *See, e.g.*, paragraphs [0091] and [0092].

At the time of the invention, it was well-established that pH constituted a natural modulator of neuronal activity. *See* abstract of Chesler, M., Kaila, K. (1993), Modulation of pH by neuronal activity, *Trends Neurosci.* 15(10):396-402 (enclosed). Thus, the Applicants’ specification, taken with the knowledge of one skilled in the art at the time this application was filed, teaches that TASK protein function is associated with neuronal activity.

Moreover, it was also well established at the time this application was filed that the activity of K^+ channels significantly influenced neuronal death/survival. For example, it had been shown that the administration of K^+ channel openers before ischemia protect neuronal cells against degeneration. *See* Heurteaux, C., *et al.* (1993), K^+ channel openers prevent global ischemia-induced expression of *c-fos*, *c-jun*, heat shock protein, and amyloid β -protein precursor genes and neuronal death in rat hippocampus, *Proc. Natl. Acad. Sci. U.S.A.* 90:9431-9435 (enclosed). It had also been shown that neurons die by apoptosis when cultured in a medium containing a physiological concentration of K^+ , and that K^+ rich depolarizing culture

medium as well as K⁺ channel blockers promote neuronal survival *in vitro*. See Yu, S.P., *et al.* (1997), Mediation of Neuronal Apoptosis by Enhancement of Outward Potassium Current, *Science* 278: 114-117 (enclosed). Thus, the Applicants' specification, taken with the knowledge of one skilled in the art at the time this application was filed, teaches that TASK protein is associated with neuronal death/survival, and consequently is useful in the treatment of nervous system diseases like epilepsy and neurodegenerative diseases, especially those associated with ischemia or anoxia.

The Office Action states on pg. 6 that, "at the time of filing, no specific association of TASK with any disease was known in the prior art nor the specification as originally filed." As discussed above, the Applicants specification does, in fact, disclose a specific association of the claimed TASK proteins with certain neurological diseases. The role of the claimed TASK proteins in neuronal cell death/survival identified in the Applicants' specification has been confirmed by the inventors, who established that TASK protein plays an important role in K⁺-dependent apoptosis of cerebellar granule neurons in culture. See Lauritzen, I., *et al.* (2003) K⁺-dependent Cerebellar Granule Neuron Apoptosis, *The Journal of Biological Chemistry* 278(34):32068-32076 (enclosed).

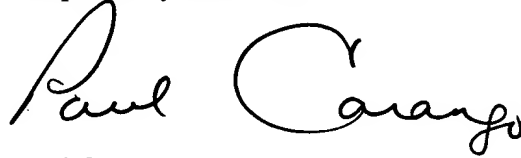
Consequently, the specification clearly establishes to those of ordinary skill in the art several utilities relating to the screening of TASK modulators and treatment of diseases of the nervous system associated with neuronal death. As such, the specification defines a "well-established utility" which is specific, substantial and credible.

The Office Action states on pg. 4 that "reliance of the utility or purported utility of others in the potassium channel class is not sufficient to establish a utility for the instantly claimed TASK channel, because the function of one member in the class of receptors does not translate into the function or utility for the rest of the members of the class." The Office Action is incorrect: The *Utility Examination Guidelines* explain that when a class of proteins is defined such that the members share a specific, substantial, and credible utility, the reasonable assignment of a new protein to the class of sufficiently conserved proteins would impute the *same* specific, substantial and credible utility to the assigned protein. 66(4) F.R. 1092, 1096, January 5, 2001. As noted by the Examiner, the assignment of the claimed TASK proteins to the class of K⁺ channels is reasonable. Thus, based on the established specific, substantial,

and credible utility of other K⁺ channels, the asserted utilities of the claimed TASK proteins are also specific, substantial and credible.

In light of the foregoing, it is respectfully requested that the rejection of claims 9-15 based on 35 U.S.C. §101 be reconsidered and withdrawn. The Applicants respectfully submit that the entire Application is now in condition for allowance, which action is respectfully requested

Respectfully submitted,

A handwritten signature in black ink that reads "Paul Carango". The signature is written in a cursive, flowing style.

Paul Carango
Reg. No. 42, 386
T. Daniel Christenbury
Reg. No. 31,750
Attorney for Applicants

TDC:rb
(215)656-3381



SCIENCE @ DIRECT

Register or Login: user name Password:

Go

Athens/Institution Login

[Home](#) [Journals](#) [Books](#) [Abstract Databases](#) [My Profile](#) [Alerts](#)[Help](#)Quick Search: within This Volume/Issue [Go](#) [Search Tips](#) WELCOME GUEST USER[results list](#) [previous](#) 14 of 17 [next](#)**Trends in Neurosciences**

Volume 15, Issue 10, 1992, Pages 396-402

doi:10.1016/0166-2236(92)90191-A [Cite or Link Using DOI](#)
Copyright © 1992 Published by Elsevier Science Ltd.**Review****Modulation of pH by neuronal activity**M. Chesler^a and K. Kaila^b^a Dept of Physiology and Biophysics and the Dept of Neurosurgery, New York University Medical Center, 550 First Avenue, New York, NY 10016, USA^b Dept of Zoology, Physiological Division, University of Helsinki, Arkadiankatu 7, SF-00100, Helsinki, Finland

Available online 5 March 2003.

This Document

- ▶ **Abstract**
- [Abstract + References](#)
- [PDF \(823 K\)](#)

Actions

- [E-mail Article](#)

Abstract

Although the requirement for a strict regulation of pH in the brain is frequently emphasized, recent studies indicate that neuronal activity gives rise to significant changes in intracellular and extracellular pH. Given the sensitivity of many ion channels to hydrogen ions, this modulation of local pH might influence brain function, particularly where pH shifts are sufficiently large and rapid. Studies using pH-sensitive microelectrodes have demonstrated marked cellular and regional variability of activity-dependent pH shifts, and have begun to uncover several of their underlying mechanisms. Accumulating evidence suggests that regional and subcellular pH dynamics are governed by the respective localization of glial cells, ligand-gated ion channels, and extracellular and intracellular carbonic anhydrase.

Trends in Neurosciences

Volume 15, Issue 10, 1992, Pages 396-402

This Document

- ▶ **Abstract**
- [Abstract + References](#)
- [PDF \(823 K\)](#)

Actions

- [E-mail Article](#)

[◀ results list](#)[◀ previous](#)

14 of 17

[next ▶](#)[Home](#)[Journals](#)[Books](#)[Abstract Databases](#)[My Profile](#)[Alerts](#)[? Help](#)[Contact Us](#) | [Terms & Conditions](#) | [Privacy Policy](#)

Copyright © 2005 Elsevier B.V. All rights reserved. ScienceDirect® is a registered trademark of Elsevier B.V.

K⁺ channel openers prevent global ischemia-induced expression of *c-fos*, *c-jun*, heat shock protein, and amyloid β -protein precursor genes and neuronal death in rat hippocampus

(Immediate early gene/*in situ* hybridization/hippocampus/transient forebrain ischemia)

CATHERINE HEURTEAUX, VALÉRIE BERTAINA, CATHERINE WIDMANN, AND MICHEL LAZDUNSKI*

Institut de Pharmacologie Moléculaire et Cellulaire, 660 route des Lucioles, Sophia Antipolis 06560 Valbonne, France

Communicated by Jean-Marie Lehn, June 1, 1993 (received for review March 8, 1993)

ABSTRACT Transient global forebrain ischemia induces in rat brain a large increase of expression of the immediate early genes *c-fos* and *c-jun* and of the mRNAs for the 70-kDa heat-shock protein and for the form of the amyloid β -protein precursor including the Kunitz-type protease-inhibitor domain. At 24 hr after ischemia, this increased expression is particularly observed in regions that are vulnerable to the deleterious effects of ischemia, such as pyramidal cells of the CA1 field in the hippocampus. In an attempt to find conditions which prevent the deleterious effects of ischemia, representatives of three different classes of K⁺ channel openers, (-)-cromakalim, nicorandil, and pinacidil, were administered both before ischemia and during the reperfusion period. This treatment totally blocked the ischemia-induced expression of the different genes. In addition it markedly protected neuronal cells against degeneration. The mechanism of the neuroprotective effects involves the opening of ATP-sensitive K⁺ channels since glipizide, a specific blocker of that type of channel, abolished the beneficial effects of K⁺ channel openers. The various classes of K⁺ channel openers seem to deserve attention as potential drugs for cerebral ischemia.

Global forebrain ischemia leads to a complete neuronal death in the CA1 field of the hippocampus after 7 days of recovery, whereas the adjacent CA3 sector and the dentate gyrus are largely more resistant (1, 2). The main factors involved in the damage of neuronal tissue following ischemia are ATP depletion (3), intracellular acidosis (4), enhanced release and/or diminished reuptake of the excitatory transmitters glutamate and aspartate (5), generation of free radicals (6), and increased Ca²⁺ influx and K⁺ efflux (7, 8).

N-Methyl-D-aspartate (NMDA) antagonists and Ca²⁺ channel blockers have exhibited little ability to reduce tissue damage in animals with global ischemia (7, 9). They seem to be more helpful in focal ischemia (10, 11). Until now antagonists of α -amino-3-hydroxy-5-methylisoxazolepropionate have been considered as the best neuroprotective agents against global brain injury (12, 13). A new class of drugs has recently attracted considerable interest for protection of the ischemic heart. This is the family of ATP-sensitive K⁺ channel (K_{ATP} channel) openers (KCOs). These molecules, including (-)-cromakalim, pinacidil, nicorandil, and RP 49356, are potent vasorelaxant and cardioprotective agents (for reviews see refs. 14-16). The cardioprotective effects of these drugs are completely reversed by antidiabetic sulfonylureas such as glibenclamide, which are blockers of K_{ATP} channels (17, 18).

K_{ATP} channels are present in the brain (19-21) and are particularly abundant in hippocampal structures, known to be vulnerable to the deleterious effects of ischemia. These

channels are activated by the same KCOs that activate cardiac K_{ATP} channels (22). Therefore it appeared worthwhile to analyze whether the KCOs can prevent the expression of the immediate early genes *c-fos* and *c-jun* and the genes encoding the 70-kDa heat-shock protein (HSP70) and amyloid β -protein precursor (APP), which are induced following global cerebral ischemia (23-30), and to determine more directly whether KCOs are neuroprotective.

MATERIALS AND METHODS

Animals. Experiments were performed on 10- to 12-week-old, 250- to 300-g male Wistar rats (Charles River Breeding Laboratories).

Drug Treatments. (-)-Cromakalim was from Beecham Pharmaceuticals, pinacidil from Leo Pharmaceuticals, and nicorandil from Rhône-Poulenc Rorer. KCOs (10 nmol/5 μ l) were administered intracerebroventricularly 30 min before the induction of cerebral ischemia and once each day during the recovery period. These doses of KCOs are similar to those previously shown to prevent seizures (31). Glipizide (1 μ mol/5 μ l; Pfizer Diagnostics) was injected intracerebroventricularly 20 min prior to openers. Control experiments were performed with intracerebroventricular injection of 0.9% NaCl under conditions used for openers.

Cerebral Ischemia Model. Forebrain ischemia involved occlusion of all four major extracranial arteries ("four-vessel occlusion" model) (2).

The first day, the rats were anesthetized by inhalation of 2% halothane mixed with 30% oxygen/70% nitrous oxide. Body temperature was maintained at 37°C. The vertebral arteries were irreversibly occluded by electrocoagulation. After a delay of 1 day for recovery, both common carotid arteries were clamped during 20 min in awake and spontaneously ventilating animals. Rats lost their righting reflex within 1 min of carotid clamping. Pharmacological treatments were administered 30 min prior to forebrain ischemia by an injection needle that was lowered bilaterally into the lateral ventricle. The injection needle was connected to a Hamilton syringe (10 μ l) positioned in a micropump delivering the drug solution at a rate (1.25 μ l/min) for 4 min. Between 1 hr and 7 days after ischemia, animals were killed by transcardial perfusion with 0.9% NaCl followed by ice-cold 1% paraformaldehyde in phosphate-buffered saline (0.15 M NaCl/0.01 M sodium phosphate, pH 7.4). The dissected brains were post-fixed in the same solution for 2 hr and then immersed overnight at 4°C in phosphate-buffered saline containing 20% sucrose. Coronal frozen sections (12 μ m) at the level of the dorsal hippocampus were cut on a cryostat (Microm) at

The publication costs of this article were defrayed in part by page charge payment. This article must therefore be hereby marked "advertisement" in accordance with 18 U.S.C. §1734 solely to indicate this fact.

Abbreviations: APP, amyloid β -protein precursor; HSP, heat-shock protein; K_{ATP} channel, ATP-sensitive K⁺ channel; KCO, K_{ATP} channel opener; NMDA, N-methyl-D-aspartate.

*To whom reprint requests should be addressed.

–25°C, collected on 3-aminopropylthoxysilane-coated slides, and stored at –70°C until use.

In Situ Hybridization. Five oligodeoxynucleotide probes were used: HSP70 (30-mer), complementary to the human sequence 5'-GTCCATGGTGCTGACCAAGATGAAG-GAGAT-3' (32); *c-jun* (60-mer), complementary to the human coding sequence 5'-CGTTGACGACGCAATCGTACT-CAACCGTGGGTGACAATTGCACCAAGTACTGAAA-GACAA-3' (33); *c-fos* (45-mer), complementary to the rat sequence 5'-TTCTCGGGTTTCAACGCGGACTACGAG-GCGTCATCCTCCCGCTGC-3' (34); and two 40-mer oligonucleotides, the APP₆₉₅ and APP₇₅₁ probes, complementary to the mouse junctional sequences arising from two possible exon combinations: 5'-GCTGGCTGCTGTCGTGGGAAC-TCGGACCACCTCCTCCACG-3' (APP₆₉₅) and 5'-TCT-TGAGTAAACTTTGGGTTGACACGC TGC CACACAC-CGC-3' (APP₇₅₁) (35). Oligodeoxynucleotides complementary to *c-fos*, *c-jun*, HSP70, APP₆₉₅, and APP₇₅₁ probes were used as sense control probes. All probes were 3' end-labeled with terminal deoxynucleotidyltransferase (Boehringer) and [α -³²S]thio[dATP] (>1000 Ci/mmol, Amersham; 1 Ci = 37 GBq) to a specific activity of 1.5×10^9 cpm/mg.

Sections were prehybridized for 1 hr at room temperature in a solution containing 4× standard saline citrate (SSC) and 1× Denhardt's solution. The slides were then rinsed 10 min in 4× SSC, acetylated for 10 min with acetic anhydride (0.5 ml/200 ml of 0.1 M triethanolamine), and dehydrated. Hybridization was carried out overnight at 42°C with *c-fos* and *c-jun* probes and at 50°C with the HSP70 oligonucleotide in 50% (vol/vol) deionized formamide/10% (wt/vol) dextran sulfate/4× SSC/1× Denhardt's solution/5% (vol/vol) sodium *N*-lauroylsarcosine/20 mM dithiothreitol/20 mM sodium phosphate containing denatured salmon sperm DNA (500 µg/ml) and yeast tRNA (250 µg/ml). For each slide, 35 ml hybridization mixture containing 3×10^5 cpm of the denatured labeled oligonucleotide was used. Slides were washed in 1× SSC/20 mM dithiothreitol at 55°C twice for 30 min before dehydration and apposition to Hyperfilm- β max (Amersham) for 10 days.

PK 11195 Binding Procedure. The ligand [³H]PK 11195 was used to label brain areas where neuronal death occurs (36). Rat brains were frozen in isopentane at –48°C. Brain sections (15 µm thick) were incubated for 60 min at 4°C in 170 mM Tris-HCl buffer (pH 7.4) containing 1 nM [³H]PK 11195 (86 Ci/mmol, NEN). The nonspecific binding component was measured by incubating adjacent tissue sections in the presence of 1 mM unlabeled PK 11195. Incubation was terminated by rinsing twice for 5 min in the cold incubation buffer and twice in cold distilled water. Sections were dried, and Hyperfilm-³H (Amersham) with a set of standards (Amersham microscale) was apposed for 46 days. Local tissue concentration of [³H]PK 11195 was determined by quantitative densitometric analysis using a computerized image-analysis system (Alcatel TITN).

RESULTS

Levels of *c-fos* and *c-jun* mRNAs and of the transcriptional regulatory factors they encode, Fos and Jun, are highly increased in rat and gerbil brain following global and focal ischemia or traumatic brain injury (23–25).

Fig. 1 B–F shows the regional expression of *c-fos* and *c-jun* mRNAs in the rat hippocampus at various times of recovery following a 20-min ischemic insult. The general expression of the two probes was identical. No induction was observed in hippocampal cells of sham-control animals (Fig. 1A). The increase in *c-fos* and *c-jun* mRNAs within the dentate granule cells was first observed after 1 hr, was more pronounced at 6 hr, and had disappeared at 24 hr following ischemia. High *c-fos* and *c-jun* labeling was observed in CA3 and CA1

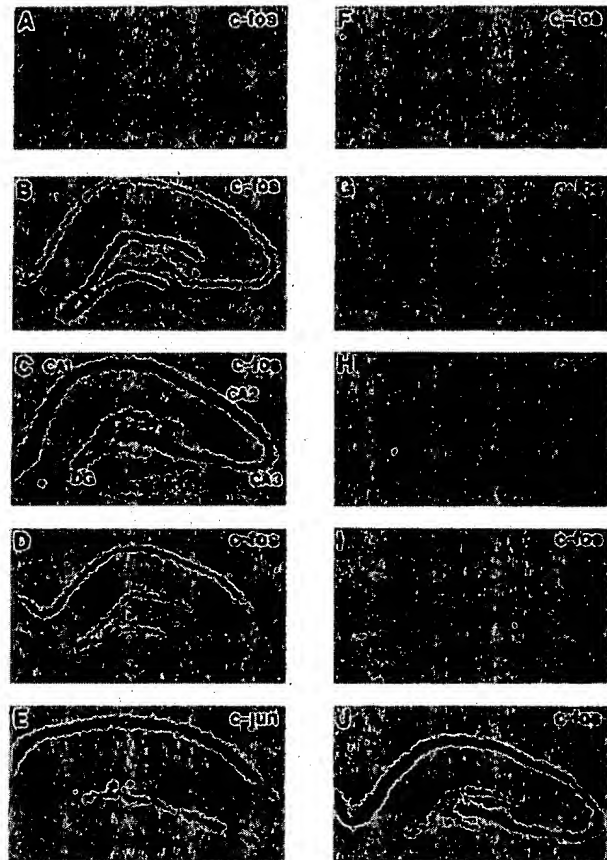


FIG. 1. Distribution of *c-fos* (A–D and F–J) and *c-jun* (E) mRNAs in rat hippocampus. Sections from saline-treated rats were obtained in sham control (A) and 1 hr (B), 6 hr (C), 24 hr (D and E), and 7 days (F) after a 20-min ischemia. Sections were obtained from (–)-cromakalim-pretreated rats 1 hr (G), 6 hr (H), and 24 hr (I) after a 20-min ischemia. Section from a rat injected with (–)-cromakalim prior to ischemia but not during 24 hr of recovery shows *c-fos* mRNA (J). Dark areas indicate high grain density. Structures devoid of labeling are white. Abbreviations are those used in the rat brain atlas of Paxinos and Watson (37). DG, dentate gyrus. (×10.)

pyramidal-cell layers at 6 hr of reperfusion and persisted only in the CA1 field at 24 hr. Total labeling disappeared by 7 days postischemia.

Injections of (–)-cromakalim (10 nmol) before the start of cerebral ischemia and during the days of recovery totally blocked the induction of ischemia-induced expression of both *c-fos* (Fig. 1 G–I) and *c-jun* (data not shown). When the drug was administered just before ischemic injury but not during reperfusion, the hybridization signal appeared at 24 hr of recovery (Fig. 1J). Like (–)-cromakalim injections, nicorandil and pinacidil injections (10 nmol) prevented the increase of both immediate early genes following global ischemia (data not shown).

HSPs play an important role in the response to stressful conditions of various cell types (for a review see ref. 38). Induction of the synthesis of HSP70 was previously observed in ischemia (26, 27).

Fig. 2 B–E shows that the regional and temporal profile of HSP70 mRNA expression after transient ischemia in rat hippocampus is the same as for *c-fos* and *c-jun*. Dentate granule cells and CA3 neurons showed transient induction of HSP70 mRNA during the first 6 hr of recovery. However, at 24 hr after ischemia only CA1 pyramidal cells demonstrated a significant hybridization, which disappeared after 7 days.

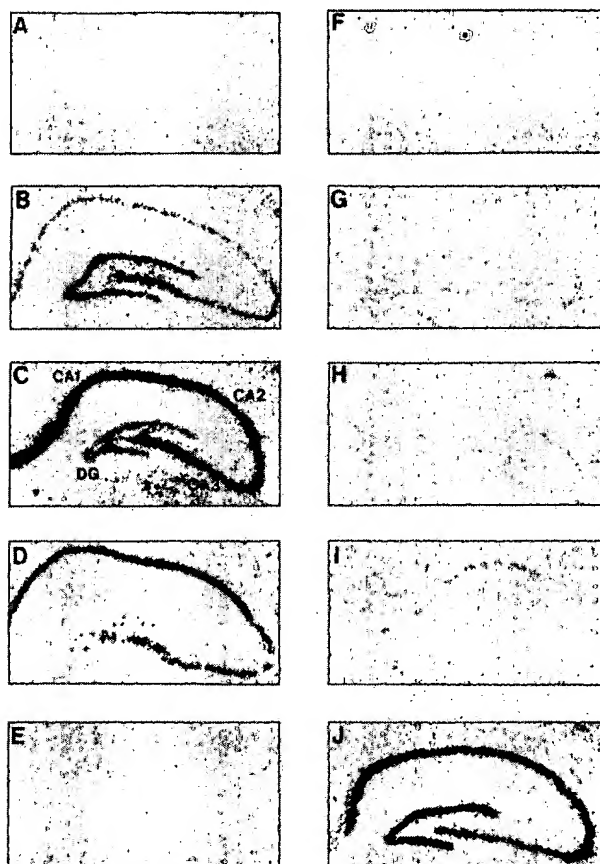


FIG. 2. Distribution of HSP70 mRNA in rat hippocampus. Sections from saline-treated rats were obtained in sham control (A) and 1 hr (B), 6 hr (C), 24 hr (D), and 7 days (E) after a 20-min ischemia. Sections were obtained at 1 hr (F), 6 hr (G), 24 hr (H), and 7 days (I) after ischemia in nicorandil-pretreated rats and at 24 hr after ischemia in a rat pretreated with a single nicorandil injection prior to ischemia (J). ($\times 10$.)

Fig. 2 F–I shows that pretreatment with nicorandil before ischemia and during recovery prevented the induction of HSP70 mRNA induced by the ischemic insult. However, a single injection of nicorandil, just before ischemia, blocked the increase in hippocampal HSP70 labeling observed after 1 and 6 hr of recovery but did not prevent a later induction of HSP70 mRNA in CA1 neurons at 24 hr (Fig. 2J).

The three isoforms of APP—APP₆₉₅, APP₇₅₁, and APP₇₇₀—are derived from alternative splicing of a single gene (35). Alterations of APP expression have previously been observed following ischemia (28, 29).

Fig. 3 shows the expression of APP₆₉₅ (B–D) and APP₇₅₁ (F–H) mRNAs in the rat hippocampus following a 20-min ischemic insult. Unlike APP₇₅₁ mRNA, which was absent in hippocampus of sham-operated rats (Fig. 3F), APP₆₉₅ mRNA was abundant in the granular layer of dentate gyrus and in pyramidal cells in layers CA1 through CA3 of control rat (Fig. 3A). The expression of APP₆₉₅ mRNA did not change after global ischemia and recovery for 7 days (Fig. 3B–D). Pretreatment with KCOs such as pinacidil had no effect (Fig. 3E). Conversely, APP₇₅₁ mRNA, which encodes the Kunitz-type protease-inhibitor domain, was induced at 24 hr post-ischemia (Fig. 3H), as previously described (39), peaked at 3 days (data not shown), and remained elevated until 7 days (Fig. 3I). KCOs such as pinacidil blocked the induction of APP₇₅₁ following global ischemia (Fig. 3J).

Fig. 4 shows more directly the neuroprotective effects of KCOs by following the appearance of peripheral-type benzo-

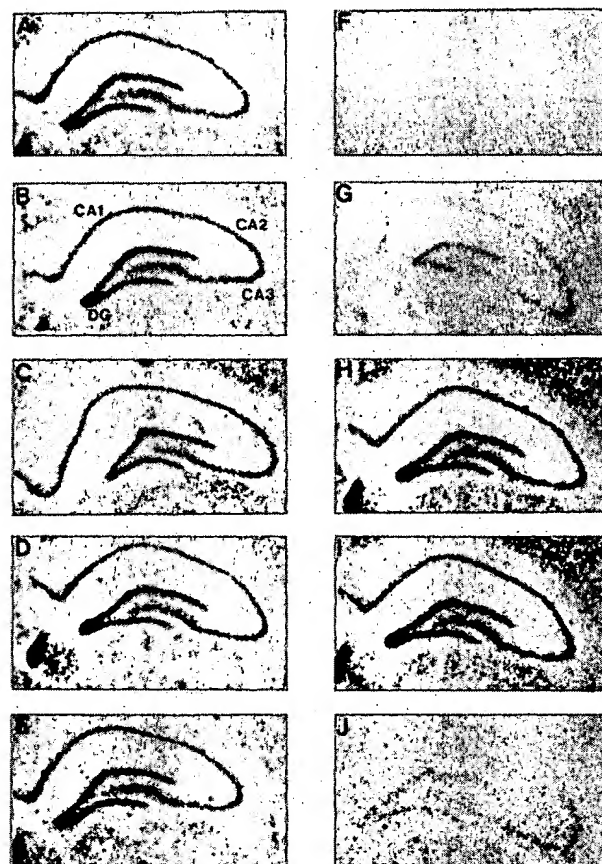


FIG. 3. Distribution of APP₆₉₅ (A–E) and APP₇₅₁ (F–J) mRNAs in rat hippocampus. Sections were obtained from saline-treated rats in sham control (A and F) and 1 hr (B and G), 24 hr (C and H), and 7 days (D and I) after 20 min of ischemia. Sections were obtained from a pinacidil-pretreated rat 7 days after ischemia (E and J). ($\times 10$.)

diazepine binding sites, which are associated with reactive astroglia and macrophage invasion following an ischemic insult and which provide an excellent marker of neuronal degeneration (36). After an ischemic insult of 20 min and 7 days of recovery, an increase in [³H]PK 11195 binding was particularly observed in the pyramidal-cell layer of the CA1 field and the hilus (Fig. 4 B and D). Pretreatment with (–)-cromakalim reduced the ischemia-induced increase of [³H]PK 11195 binding and thus protected against ischemia-induced loss of CA1 pyramidal cells (Fig. 4 C and D). Counting of intact cells and density of neurons on histologic sections showed that delayed neuronal death was observed in 78% of CA1 neurons 7 days after ischemia and that 65% of the CA1 cells survived at 7 days of reperfusion after KCO treatment.

Since the sulfonylurea glipizide is a potent blocker of K_{ATP} channels after they have been activated by KCOs (22), we analyzed the effect of glipizide on the protection provided by (–)-cromakalim. For each probe used (*c-fos*, *c-jun*, HSP70, APP), glipizide completely antagonized the effect of KCOs on the induction of expression following ischemic injury. Fig. 5A shows that a hippocampal expression of HSP70 mRNA could be induced, as in the control (Fig. 2B), 1 hr after ischemia if glipizide had been injected prior to (–)-cromakalim (before ischemia), whereas, as previously observed, HSP70 induction was totally prevented by injection of the KCO alone (Fig. 5B).

DISCUSSION

KCOs are mainly known for their vasorelaxant activities and for their use as antihypertensive agents (14–16). The bene-

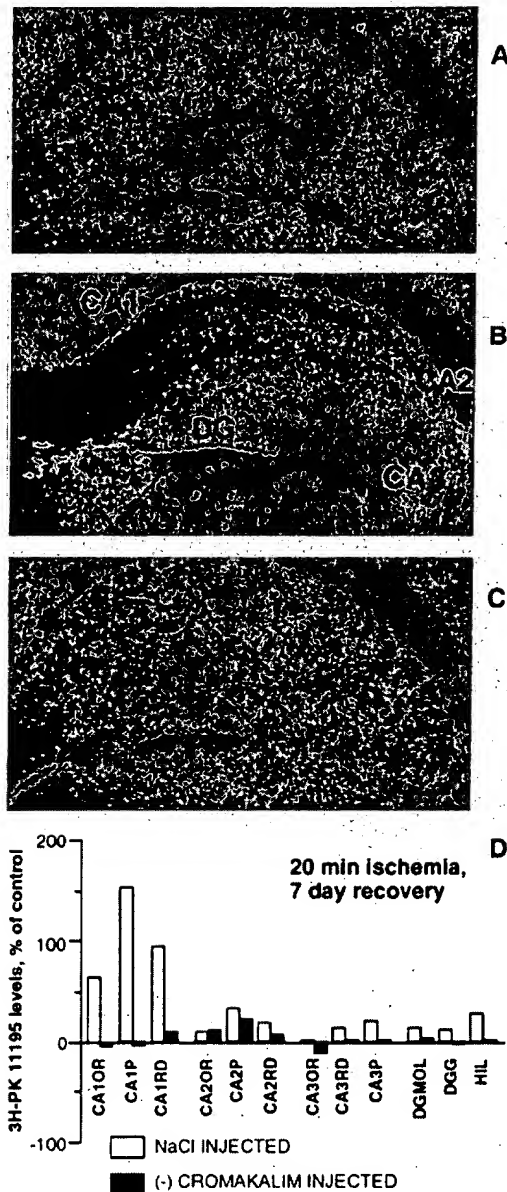


FIG. 4. Distribution of [3 H]PK 11195 binding in rat hippocampus. (A–C) Sections were obtained from saline-treated rats in sham control (A) and 7 days after a 20-min ischemia and from a (–)-cromakalim-pretreated rat 7 days after ischemia (C). ($\times 23$.) (D) Computerized image analysis of autoradiographs giving averages of the percentage of [3 H]PK 11195 binding at 7 days of recovery in (–)-cromakalim-pretreated (filled bars) and saline-pretreated (open bars) rat hippocampus. These data are means \pm SD of optical density determination, calculated from 20 bilateral measurements on four sections per animal in the three rats of each experimental group. Variations were assessed with a two-tailed Student *t* test. Abbreviations are those used in ref. 37: OR, stratum oriens; P, stratum pyramidale; RD, stratum radiatum; DGMOL and DGG, molecular and granule layers of dentate gyrus; HIL, hilus of dentate gyrus.

ficial effects are linked to the induction of a hyperpolarization of the smooth muscle that prevents excessive Ca^{2+} entry.

(–)-Cromakalim, pinacidil, and RP 49356 have also been shown to open K_{ATP} channels in cardiac myocytes (ref. 40; reviewed in refs. 14–16). Their action is associated with a shortening of the cardiac action potential that (i) prevents Ca^{2+} entry that would normally occur during the plateau phase and, (ii) consequently, decreases the consumption of ATP which is necessary in normal conditions for the various

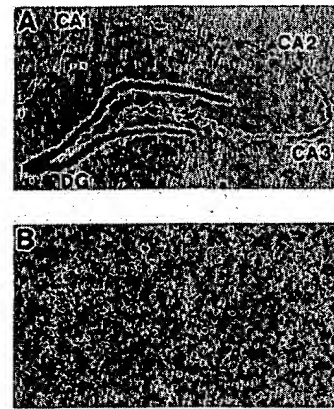


FIG. 5. HSP70 mRNA induction following global ischemia and 1 hr of recovery. (A) Rat injected with glipizide 20 min prior to (–)-cromakalim administration. (B) Rat injected with (–)-cromakalim.

Ca^{2+} pumps in charge of maintaining a low intracellular Ca^{2+} concentration. Saving ATP and preventing excessive Ca^{2+} entry are two important properties for potential drugs in the treatment of cardiac ischemia. It is therefore not surprising that (–)-cromakalim, pinacidil, and RP 52891 are capable of reducing ischemic injury (41).

K_{ATP} channels are present in the brain (19–21) with high density in substantia nigra, globus pallidus, cerebellum, and hippocampus. They are sensitive to external concentrations of glucose (42) and are opened by anoxia (20, 22, 43). They are also opened by KCOs (22). They are present in hippocampus both presynaptically and postsynaptically (44–47) and are particularly situated in mossy fibers which are associated with glutamate release (48).

Brain ischemia is associated with an excessive extracellular level of glutamate (5), probably mainly due to the fact that the high intracellular Na^+ concentration produced by ischemia prevents glutamate reuptake (after it has been liberated) through the glutamate- Na^+ cotransporter (49). On the other hand, an important extracellular glutamate concentration will produce a strong stimulation of NMDA receptors and an increased Ca^{2+} entry into target neurons that will be responsible for neuronal death (5, 7).

Two important properties can be expected from KCOs: (i) they should hyperpolarize synaptic terminals and thus massively prevent Ca^{2+} entry and consequently glutamate release (22, 42, 46) and (ii) they should hyperpolarize glutamate-sensitive neurons, thus conferring resistance to the depolarization induced by the various glutamate receptors and preventing the relief of the Mg^{2+} block of the NMDA receptor channel, which is known to be voltage-dependent and facilitated by a depolarization (50). For all these reasons KCOs should be expected to have a protective action against ischemia.

The deleterious effects of ischemia are associated with the induction of expression of mRNAs encoding the Fos and Jun nuclear proteins (23–25). Forebrain global ischemia produced an induction of these immediate early genes which at 24 hr postischemia remained intense only in the hippocampal CA1 field.

HSPs, and particularly HSP70, are synthesized in a variety of stress-related conditions, including transient ischemia (26, 27). Both temporal and spatial patterns of HSP70 mRNA induced expression following ischemia have been found in this work to be similar to expression patterns of *c-fos* and *c-jun*. The expression of *c-fos*, *c-jun*, and HSP70 mRNA was prevented by treatment with KCOs before ischemia and by treatment during reperfusion, indicating that these drugs

abolish the stress effects created by the ischemic insult. When the drug is injected only before ischemia and not during recirculation, KCOs are neuroprotective just for 1 day.

Many studies have shown the expression of APP following injuries of the central nervous system (28, 29, 51). One of the APP forms is APP₇₅₁, which contains a 56-amino acid domain very homologous to the Kunitz family of serine protease inhibitors (51). The other molecular form, APP₆₉₅, which derives from alternative splicing of the APP gene, does not contain this Kunitz inhibitor-like domain (35). The transcriptional expression of APP₆₉₅ was not affected by ischemia, whereas the level of mRNA for APP₇₅₁ was greatly increased 24 hr after ischemia, as also was observed by Northern blot analyses (39). This increase occurred in granule cells of the dentate gyrus and in pyramidal cells of CA1 and CA3 fields and it persisted in the CA1 region until 7 days after ischemia. Pinacidil injected before ischemia clearly blocked the expression of APP₇₅₁.

All these results taken together show that the different types of KCOs prevent the ischemia-induced expression of very different genes. They are in complete agreement with results involving cell counting in the CA1 sector or [³H]PK 11195 as a marker of cell death (36).

One of the important properties of K_{ATP} channels is that, once they have been opened (e.g., by KCOs), they can be blocked with high potency by sulfonylureas such as glibenclamide or glipizide (17, 18, 22, 40, 42, 47, 52, 53). Indeed the beneficial effects of KCOs against the series of events produced by ischemia were suppressed when openers were administered in the presence of glipizide before ischemia was started.

In conclusion, this work shows beneficial effects of KCOs against global ischemia, as previously suggested (22). These effects are due to the action of these different compounds on K_{ATP} channels (probably at both pre- and postsynaptic levels). To find a practical application for these observations in drug therapy, it will be necessary (i) to synthesize KCOs which pass the blood-brain barrier and (ii) to develop openers with an increased specificity for brain K_{ATP} channels, to avoid effects of these compounds on blood pressure. This seems to be feasible, since K_{ATP} channels in brain and in vascular smooth muscle belong to different subtypes (54). Moreover, it is probable that KCOs will work better in hypoxic or ischemic than in normoxic conditions, since their action is known to be facilitated in the presence of ADP (52, 55).

The mechanisms by which KCOs prevent the deleterious effects of ischemia are probably similar to those which make them potentially useful compounds against various types of epileptic seizures (31, 56). Because this class of compounds prevents the expression of mRNAs related to APP, it might be interesting to investigate whether they would also be useful in preventing the development of amyloid accumulation in Alzheimer disease itself.

We thank G. Jarretou, F. Aguila, and C. Roulinat for expert technical assistance and Dr. Plotkine and his lab for useful advice on ischemia methods. This work was supported by the Centre National de la Recherche Scientifique and the Fondation pour la Recherche Médicale.

1. Ito, U., Spatz, M., Walker, J. T., Jr., & Klatzo, I. (1975) *Acta Neuropathol.* 32, 209–223.
2. Pulsinelli, W. A. & Brierley, J. B. (1979) *Stroke* 10, 267–272.
3. Siesjö, B. K. (1978) in *Brain Energy Metabolism*, ed. Siesjö, B. K. (Wiley, New York).
4. Siesjö, B. K. (1988) *Neurochem. Pathol.* 9, 31–88.
5. Benveniste, H., Drejer, J., Schousboe, A. & Diemer, N. H. (1984) *J. Neurochem.* 43, 1369–1374.
6. Kontos, H. A. & Wei, E. P. (1986) *J. Neurosurg.* 64, 803–807.

7. Siesjö, B. K. & Bengtsson, F. (1989) *J. Cereb. Blood Flow Metab.* 9, 127–140.
8. Nicholson, C., Bruggencate, G. T., Steinberg, R. & Stöckle, H. (1977) *Proc. Natl. Acad. Sci. USA* 74, 1287–1290.
9. Buchan, A., Hui, L. & Pulsinelli, W. A. (1991) *J. Neurosci.* 11, 1049–1056.
10. Zivin, J. A. & Choi, D. W. (1991) *Sci. Am.* 265, 36–43.
11. Takakura, S., Susumu, T., Satoh, H., Mori, J., Shiino, A. & Handa, J. (1991) *Jpn. J. Pharmacol.* 56, 547–550.
12. Sheardown, M. J., Nielsen, E. O., Hansen, A. J., Jacobsen, P. & Honoré, T. (1990) *Science* 247, 571–574.
13. Nellgard, B. & Wieloch, T. (1992) *J. Cereb. Blood Flow Metab.* 12, 2–6.
14. Edwards, G. & Weston, A. H. (1990) *Trends Pharmacol. Sci.* 11, 417–422.
15. Escande, D. & Caverio, I. (1992) *Trends Physiol. Sci.* 13, 269–272.
16. Quast, U. (1992) *Fundam. Clin. Pharmacol.* 6, 279–293.
17. Schmid-Antomarchi, H., De Weille, J. R., Fosset, M. & Lazdunski, M. (1987) *J. Biol. Chem.* 262, 15840–15844.
18. Fosset, M., De Weille, J. R., Green, R. D., Schmid-Antomarchi, H. & Lazdunski, M. (1988) *J. Biol. Chem.* 263, 7933–7936.
19. Ashford, M. L., Sturgess, N. C., Traut, N. J., Gardner, N. J. & Hales, C. N. (1988) *Pflügers Arch.* 412, 297–304.
20. Mourre, C., Ben, Ari, Y., Bernardi, H., Fosset, M. & Lazdunski, M. (1989) *Brain Res.* 486, 159–164.
21. Mourre, C., Widmann, C. & Lazdunski, M. (1990) *Brain Res.* 519, 29–43.
22. Schmid-Antomarchi, H., Amoroso, S., Fosset, M. & Lazdunski, M. (1990) *Proc. Natl. Acad. Sci. USA* 87, 3489–3492.
23. Uemura, Y., Kowall, N. W. & Beal, M. F. (1991) *Brain Res.* 542, 343–347.
24. Wessel, T. C., Tong, H. J. & Volpe, B. T. (1991) *Brain Res.* 567, 231–240.
25. Jorgensen, M. B., Deckert, J., Wright, D. C. & Gehlert, D. R. (1989) *Brain Res.* 484, 393–398.
26. Nowak, T. S., Jr. (1991) *J. Cereb. Blood Flow Metab.* 11, 432–439.
27. Kawagoe, J., Abe, K. & Kogure, K. (1992) *Brain Res.* 599, 197–203.
28. Stephenson, D. T., Rash, K. & Clemens, J. A. (1992) *Brain Res.* 593, 128–135.
29. Wakita, H., Tomimoto, H., Akiguchi, I., Ohnishi, K., Nakamura, S. & Kimura, J. (1992) *Neurosci. Lett.* 146, 135–138.
30. Doucet, J. P., Squinto, S. P. & Bazan, N. G. (1990) *Mol. Neurobiol.* 4, 27–55.
31. Gandolfo, G., Romettino, S., Gottesmann, C., Van Luitelaar, G., Coenen, A., Bidard, J.-N. & Lazdunski, M. (1989) *Eur. J. Pharmacol.* 167, 181–183.
32. Hunt, S. & Morimoto, R. I. (1985) *Proc. Natl. Acad. Sci. USA* 82, 6455–6459.
33. Angel, P., Allegretto, E. A., Okino, S. T., Hattori, K., Boyle, W. J., Hunter, T. & Karin, M. (1988) *Nature (London)* 332, 166–171.
34. Curran, T., Gordon, M. B., Rubino, K. L. & Sambucetti, L. C. (1987) *Oncogene* 2, 79–84.
35. Yamada, T., Sasaki, H., Dohura, K., Goto, I. & Sakaki, Y. (1989) *Biochem. Biophys. Res. Commun.* 158, 906–912.
36. Benavides, J., Capdeville, C., Dauphin, F., Dubois, A., Duverger, D., Fage, D., Gotti, B., MacKenzie, E. T. & Scatton, B. (1990) *Brain Res.* 522, 275–289.
37. Paxinos, G. & Watson, C. (1982) *The Rat Brain in Stereotaxic Coordinates* (Academic, New York), pp. 54–56.
38. Welch, W. J. (1992) *Physiol. Rev.* 72, 1063–1081.
39. Abe, K., Tanzi, R. E. & Kogure, K. (1991) *Neurosci. Lett.* 125, 172–174.
40. Escande, D., Thuringer, D., Leguern, S. & Caverio, I. (1988) *Biochem. Biophys. Res. Commun.* 154, 620–625.
41. Grover, G. J., Dzwonczyk, S. & Sleph, P. G. (1990) *Eur. J. Pharmacol.* 191, 11–18.
42. Amoroso, S., Schmid-Antomarchi, H., Fosset, M. & Lazdunski, M. (1990) *Science* 247, 852–854.
43. Jiang, C. & Haddad, G. G. (1989) *J. Neurophysiol.* 66, 103–111.
44. Ben Ari, Y. & Lazdunski, M. (1989) *Eur. J. Pharmacol.* 165, 331–332.
45. Ben Ari, Y., Krnjevic, K. & Crepel, V. (1990) *Neuroscience* 37, 55–60.
46. Abele, A. E. & Miller, R. J. (1990) *Neurosci. Lett.* 115, 195–200.
47. Politi, D. M. T. & Rogawski, M. A. (1991) *Mol. Pharmacol.* 40, 308–315.
48. Mourre, C., Widmann, C. & Lazdunski, M. (1991) *Brain Res.* 540, 340–344.
49. Nicholls, D. & Attwell, D. (1990) *Trends Pharmacol. Sci.* 11, 462–468.
50. Ascher, P. & Nowak, L. (1987) *Trends Neurosci.* 10, 284–288.
51. Tanzi, R. E., McClatchey, A. I., Lamperti, E. D., Gusella, J. F. & Neve, R. L. (1988) *Nature (London)* 331, 528–530.
52. Dunne, M. J. & Petersen, O. H. (1991) *Biochim. Biophys. Acta Rev. Biomembr.* 1071, 67–82.
53. Häusser, M., De Weille, J. R. & Lazdunski, M. (1991) *Biochem. Biophys. Res. Commun.* 174, 909–914.
54. Miller, R. J. (1990) *Trends Neurosci.* 13, 197–199.
55. Allard, B. & Lazdunski, M. (1992) *Pflügers Arch.* 422, 185–192.
56. Alzheimer, C. & Ten Bruggencate, G. (1988) *Naunyn-Schmiedeberg Arch. Pharmacol.* 337, 429–434.

Mediation of Neuronal Apoptosis by Enhancement of Outward Potassium Current

Shan Ping Yu, Chen-Hsiung Yeh, Stefano L. Sensi,
Byoung J. Gwag, Lorella M. T. Canzoniero,
Z. Shadi Farhangrazi, Howard S. Ying, Min Tian,
Laura L. Dugan, Dennis W. Choi*

Apoptosis of mouse neocortical neurons induced by serum deprivation or by staurosporine was associated with an early enhancement of delayed rectifier (I_K) current and loss of total intracellular K^+ . This I_K augmentation was not seen in neurons undergoing excitotoxic necrosis or in older neurons resistant to staurosporine-induced apoptosis. Attenuating outward K^+ current with tetraethylammonium or elevated extracellular K^+ , but not blockers of Ca^{2+} , Cl^- , or other K^+ channels, reduced apoptosis, even if associated increases in intracellular Ca^{2+} concentration were prevented. Furthermore, exposure to the K^+ ionophore valinomycin or the K^+ -channel opener cromakalim induced apoptosis. Enhanced K^+ efflux may mediate certain forms of neuronal apoptosis.

Neurons undergo apoptosis during normal development and in certain disease states (1). Elevated extracellular K^+ interdicts this death (2, 3), an effect attributed to increasing Ca^{2+} influx through voltage-gated Ca^{2+} channels, thus increasing intracellular Ca^{2+} concentration ($[Ca^{2+}]_i$) toward a set point that is optimal for survival (3). The antiapoptotic effect of high K^+ concentration can be attenuated by removing extracellular Ca^{2+} or adding Ca^{2+} -channel blockers (3, 4), and neuronal survival can be enhanced by opening Ca^{2+} channels with dihydropyridine agonists (4, 5) or inhibiting intracellular Ca^{2+} sequestration with thapsigargin (6). However, although these data support an antiapoptotic effect of increasing $[Ca^{2+}]_i$, they do not exclude other possibilities. Furthermore, increases in $[Ca^{2+}]_i$ can induce apoptosis under some conditions (7), and, in the absence of nerve growth factor, a high concentration of K^+ promoted survival of sympathetic neurons without an increase in $[Ca^{2+}]_i$ (8).

To test the idea that high extracellular K^+ might also attenuate neuronal apoptosis by reducing K^+ efflux, we first examined whether neurons undergoing apoptosis exhibited an up-regulation of outward K^+ currents. Cultured mouse cortical neurons in mixed (neurons and glia) or near-pure neuronal cultures (9, 10) were studied with whole-cell recording between 7 and 12 days in vitro (DIV) (11). A persistent outward current, consistent with the delayed rectifier I_K (Fig. 1A), and a transient outward

current, consistent with I_A (Fig. 1B) (12), were the two major voltage-gated K^+ currents observed. I_K was reduced by increasing extracellular K^+ (Fig. 1C) and exhibited slow kinetics, outward rectification, and sensitivity to tetraethylammonium (TEA) (Fig. 1A) (13). I_A exhibited rapid activation and inactivation as well as sensitivity to 4-aminopyridine (4AP) (Fig. 1B). A small inward rectifier current activated with hyperpolarization and a small outward current consistent with the ATP-sensitive K^+ current (K_{ATP}) was also observed. Other major K^+ currents, the M-current (I_M) and the Ca^{2+} -dependent, high-conductance K^+ current (BK current), were not detected.

In seven to nine DIV neurons in neuronal cultures, the steady-state current of I_K activated by voltage jump from -70 to $+40$ mV was 506 ± 46 pA ($n = 25$ cells, mean \pm SEM). Six hours after serum withdrawal, I_K at $+40$ mV was increased by 61%

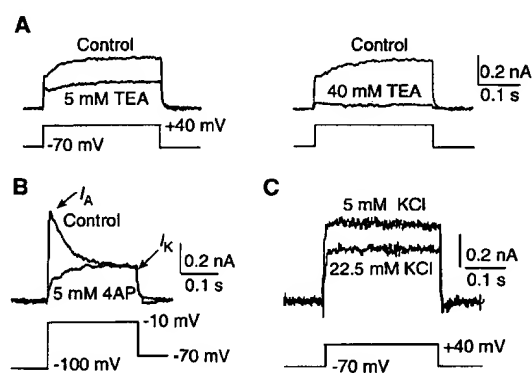
and the maximal K^+ conductance more than doubled without change in voltage sensitivity or kinetics (Fig. 2, A, C, and D; Table 1). Holding current at -70 mV shifted from -18 ± 6 pA at baseline to -2 ± 4 pA after 5 hours of serum deprivation ($P < 0.05$; $n = 44$ and 23, respectively), indicative of membrane hyperpolarization. Cell capacitance gradually decreased, consistent with progressive cell body shrinkage (Table 1), and total intracellular K^+ dropped by $7 \pm 3\%$ and $13 \pm 4\%$, respectively, after 5 and 9 hours in serum-free medium (both different from baseline at $P < 0.05$; $n = 10$) (14). The enhanced I_K remained sensitive to block by TEA (Fig. 2B); 5 mM TEA completely prevented loss of intracellular K^+ .

No change in I_K was seen in neurons exposed to a sham wash (Fig. 2C). The enhancement in I_K induced by serum deprivation was not blocked by cycloheximide ($1 \mu\text{g/ml}$) (Table 1), suggesting that the enhancement did not require new protein synthesis.

Neuronal apoptosis induced in mixed cultures (DIV 10 to 12) by $0.1 \mu\text{M}$ staurosporine was also associated with an enhancement in I_K . Despite an initial nonsignificant trend toward reduced I_K after 30 min, after 9 to 11 hours I_K was increased by 90% and maximum K^+ conductance was doubled (Table 1). In contrast, I_K did not change in neurons that underwent *N*-methyl-D-aspartate (NMDA)-induced excitotoxic necrosis (Table 1), although by 11 hours neurons exhibited substantial cell swelling. Furthermore, exposure to staurosporine did not alter I_K in older neurons (DIV 17; $n = 5$), which survive such exposure (15).

Serum deprivation and staurosporine exposure also altered the transient current I_A , although with opposite effects. At times of

Fig. 1. Voltage-gated K^+ currents in cultured cortical neurons. (A) Normal I_K recorded from neurons in mixed neuronal glial cultures. Current was activated by stepping from a holding potential of -70 to $+40$ mV for 300 to 600 ms, with leak current subtraction. The noninactivating outward current was dose dependently blocked by 1 to 40 mM bath-applied TEA (effects shown are 5 and 40 mM). (B) 4AP selectively blocked a transient outward K^+ current, I_A . Currents were activated by a voltage step from -100 to -10 mV. The initial transient outward current was blocked by 5 mM 4AP, consistent with I_A . The 4AP resistant current was blocked by TEA, consistent with I_K as shown in (A). (C) I_K was sensitive to extracellular K^+ concentration. When K^+ was increased from 5 to 22.5 mM, the same voltage step activated a smaller outward current, similar to the effect of 5 mM TEA. The inhibitory effect of medium with high K^+ concentration is expected from a reduced driving force for K^+ efflux, predicted by the Nernst equation.



Center for the Study of Nervous System Injury and Department of Neurology, Washington University School of Medicine, St. Louis, MO 63110, USA.

*To whom correspondence should be addressed at the Department of Neurology, Box 8111, Washington University School of Medicine, 660 South Euclid Avenue, St. Louis, MO 63110, USA. E-mail: choid@neuro.wustl.edu

Table 1. Effects of apoptotic and necrotic insults on I_K , I_{K1} , steady-state current activated by voltage step from -70 to $+40$ mV; G_{max} , maximum conductance; $V_{threshold}$, voltage threshold for I_K activation; C_M , membrane capacitance; $V_{2/1}$, voltage for I_K half activation; $\tau_{opening}$, time constant for I_K opening at $+40$ mV measured in the presence of 5 mM 4AP by single exponential curve fitting. These parameters were examined before (control)

and at plateau levels after insults: 11 hours in staurosporine (0.1 μ M), 6 hours in serum deprivation, and 11 hours in 15 μ M NMDA (plus 10 μ M glycine; DIV 10 to 12 mixed cultures). Cycloheximide concentration was 1 μ g/ml. Serum deprivation and staurosporine exposure were performed in pure neuron cultures and mixed cultures, respectively (9, 10).

	I_K (pA)	G_{max} (nS)	C_M (pF)	I_K density (pA/pF)	$V_{threshold}$ (mV)	$V_{1/2}$ (mV)	$\tau_{opening}$ (ms)
Control	506 \pm 46	4.1 \pm 0.5	31.6 \pm 2.4	25.2 \pm 6.7	-33.3 \pm 3.1	2.6 \pm 1.1	21.7 \pm 3.6
Serum deprivation	815 \pm 61*	9.7 \pm 0.2*	24.9 \pm 2.1*	47.0 \pm 4.9*	-34.5 \pm 2.5	1.6 \pm 0.9	28.8 \pm 3.3
Control	512 \pm 81	4.6 \pm 0.6	32.0 \pm 2.8	15.2 \pm 2.6	-33.0 \pm 3.2	2.5 \pm 1.0	22.1 \pm 3.5
Staurosporine	969 \pm 145*	9.8 \pm 2.6*	23.9 \pm 2.0*	31.8 \pm 7.2*	-38.1 \pm 1.0*	-2.1 \pm 0.6*	25.9 \pm 4.0
Control	361 \pm 59	—	—	—	—	—	—
Serum deprivation + cycloheximide	760 \pm 149*	—	—	—	—	—	—
Control	597 \pm 97	—	—	—	—	—	—
NMDA	565 \pm 151	—	—	—	—	—	—

*Significant difference ($P < 0.05$) from respective control by t -test; $n = 5$ to 25 (most $n \geq 10$).

maximal change, serum deprivation (6 hours) increased I_A by 28% ($P < 0.05$; $n = 20$), whereas staurosporine (0.1 μ M; 9 hours) decreased I_A by 75% ($P < 0.05$; $n = 8$). Exposure to NMDA did not alter I_A . Because activity of voltage-gated Ca^{2+} channels may affect apoptosis, we monitored high-voltage-activated (HVA) Ca^{2+} currents during serum deprivation and found no significant change (232 ± 35 pA in control cells, 192 ± 33 and 147 ± 51 pA after 6 and 9 hours; $P = 0.43$ and 0.22 , respectively; $n = 5$ per condition). Tested after 5 to 9 hours in 0.1 μ M staurosporine, the I_M and BK currents remained undetectable; the inward rectifier and K_{ATP} current were not altered.

The selective enhancement of I_K induced by either serum deprivation or staurosporine exposure, as well as the increase in I_A induced by the former, occurred be-

fore development of neuronal apoptotic death (16), consistent with a critical early role. In support of this idea, adding 1 to 5 mM TEA or increasing extracellular K^+ from 5 to 25 mM reduced both forms of apoptosis (Fig. 3, A and B). In contrast, neither the TEA analog tetramethylammonium (5 mM; inactive on I_K) nor 4AP (5 mM; antagonist for the slowly inactivating K^+ current I_D as well as I_A) was effective (Fig. 3B). Other antagonists that targeted K_{ATP} (tolbutamide; 100 to 500 μ M) or the SK channel (apamin; 1 μ M) also lacked protective effect. TEA may inhibit Cl^- currents in cortical neurons (17); however, no neuroprotection was observed with the Cl^- -channel antagonist anthracene-9-carboxylic acid (500 μ M) (data not shown).

We considered the possibility that the protective effect of TEA was mediated by an increase in $[Ca^{2+}]_i$. Neuronal $[Ca^{2+}]_i$

measured with fura-2 (18) was about 100 nM at rest and increased to a plateau value of about 200 nM after 1 to 2 hours of exposure to 5 mM TEA or 25 mM K^+ . Gadolinium (2 to 10 μ M), which completely blocked the HVA Ca^{2+} current (Fig. 4A), kept $[Ca^{2+}]_i$ at resting level during 2 to 16 hours of exposure to TEA or 25 mM K^+ (Fig. 4B); neither gadolinium (Fig. 4C) nor the L-type Ca^{2+} -channel antagonist nifedipine (5 μ M; Fig. 4D) blocked the anti-apoptotic effects. Neither gadolinium nor nifedipine showed neuroprotection when applied alone (Fig. 4, B and C).

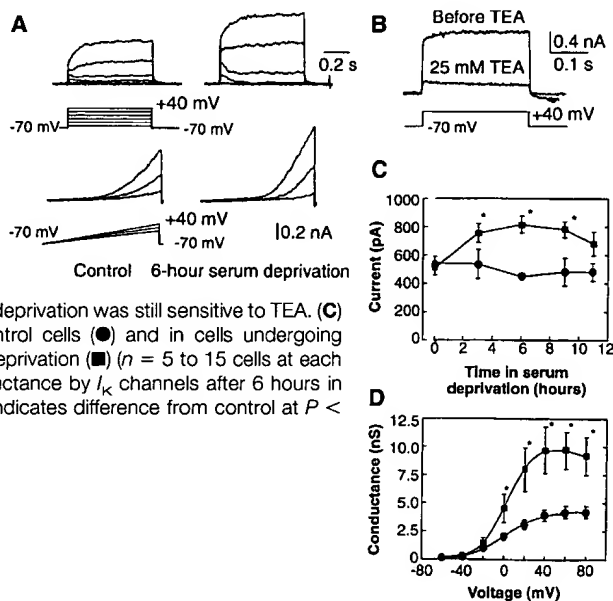
We considered the possibility that membrane depolarization might mediate the anti-apoptotic effects of TEA or high K^+ concentration. However, the Na^+ -channel opener veratridine, which depolarized the membrane from control -51 ± 2 mV ($n = 45$) to -30 ± 2 mV ($n = 21$), similar to the membrane depolarization by 5 mM TEA (-34 ± 4 mV; $n = 15$), increased staurosporine-induced neuronal cell death (Fig. 3B).

In support of the hypothesis that increased K^+ efflux might be a primary step leading to apoptosis, application of the selective K^+ ionophore valinomycin (19) triggers apoptosis in thymocytes, lymphocytes, and tumor cells (20). Exposure to 20 nM valinomycin for 24 to 48 hours induced typical neuronal apoptosis in cortical cultures, characterized by chromatin condensation, cell body shrinkage, internucleosomal DNA fragmentation, and sensitivity to cycloheximide (1 μ g/ml) or the caspase inhibitor Z-Val-Ala-Asp-fluoromethylketone (100 μ M) (zVAD; Fig. 5). Furthermore, 24 to 48 hours of exposure to the K^+ -channel opener cromakalim, which activates K_{ATP} channels as well as I_K -like currents in mammalian central neurons (21), also induced typical neuronal apoptosis (Fig. 5).

In summary, four arguments suggest that a long-lasting enhancement of outward K^+

Fig. 2. Enhancement of I_K

by serum deprivation. (A) (Left) Recordings from DIV 9 neurons in pure neuronal cultures showing the I - V relationship of I_K as revealed by rectangular and ramp voltage steps. (Right) After 6 hours of serum deprivation, the same voltage steps triggered much larger currents and outward rectification. (B) The I_K enhanced by serum deprivation was still sensitive to TEA. (C) Change in I_K with time in control cells (●) and in cells undergoing apoptosis induced by serum deprivation (■) ($n = 5$ to 15 cells at each point). (D) Increased K^+ conductance by I_K channels after 6 hours in serum-free medium. Asterisk indicates difference from control at $P < 0.05$ by t -test.



current is a key mediator of the forms of cortical neuronal apoptosis studied here. First, augmentation in I_K and loss of neuronal cell K^+ occurred early in the course of neuronal apoptosis, well before the commit-

ment point (16). The magnitude of this increase in K^+ current is comparable with that associated with mitogenesis (22) and proliferation (23) in several cell types (~0.5- to 3-fold increases of peak outward

K^+ current). Second, this I_K augmentation was specific to apoptosis but not triggered by necrotic insult or in older cells resistant to apoptosis. Third, blocking of this I_K enhancement and cellular K^+ depletion by TEA or by increasing extracellular K^+ prevented apoptosis. Finally, increasing membrane K^+ permeability by adding either the ionophore valinomycin or the endogenous K^+ -channel opener cromakalim sufficed to induce neuronal apoptosis.

In isolation, the third argument stated above is unsurprising, because both TEA and raising extracellular K^+ increase neuronal excitation and $[Ca^{2+}]_i$, and thus reduced apoptosis would be predicted by the Ca^{2+} set-point hypothesis. However, neuroprotection was maintained even when associated increases in $[Ca^{2+}]_i$ were completely blocked. Some membrane-associated signaling proteins such as adenylyl cyclase may be voltage sensitive (24), but comparable membrane depolarization induced by veratridine was not neuroprotective.

Involvement of K^+ efflux in apoptosis has intuitive appeal, because loss of cell volume is a cardinal feature of apoptosis, and K^+ extrusion is a plausible mechanism to achieve this loss (25). The I_A blocker 4AP recently has been reported to inhibit the shrinkage of human eosinophils undergoing cytokine deprivation-induced apo-

Fig. 3. Prevention of apoptosis by I_K blocker TEA or by raising extracellular K^+ concentration. Pure neuronal culture (DIV 7 to 9) in 24-well plates was used for serum deprivation because the presence of glia prevents neuronal degeneration after serum deprivation. Mixed culture containing neurons and a glia bed (DIV 10 to 12) was used for exposure to staurosporine (0.1 μ M). NMDA receptor antagonist 1 μ M dizocilpine maleate ((+)-5-methyl-10,11-dihydro-5H-dibenzo[a,d]cyclohepten-5,10-imine (MK-801)) and non-NMDA receptor blocker 2,3-dihydro-6-nitro-7-sulfamoylbenzo(f)quinoline (5 μ M) were added to block glutamate excitotoxicity in serum-deprivation experiments. Neuronal death was detected 24 and 48 hours after apoptotic insult. (A) (Left) Phase-contrast micrograph of a pure neuronal culture 48 hours after onset of serum deprivation, showing widespread neuronal apoptosis. (Right) Preservation of neurons in serum-free medium in the presence of 5 mM TEA. Bar = 50 μ m. (B) Neuronal apoptosis, expressed as a fraction of the total number of neurons, induced by 48 hours of exposure to serum deprivation (left) or 0.1 μ M staurosporine (right), either alone or in the presence of the indicated bath-applied drug (mean \pm SEM; n = 4 to 16 cultures per condition). Serum-deprivation-induced cell death was assessed by cell counts after staining with 0.4% trypan blue dye. For staurosporine experiments, cell death was measured by lactate dehydrogenase released into the medium (30). Cell deaths by both insults were assayed alternatively by two methods and similar results were obtained. Higher concentrations of TEA (20 mM) were toxic. Asterisk indicates significant difference from the control at P < 0.05 by t -test with Bonferroni correction for four comparisons.

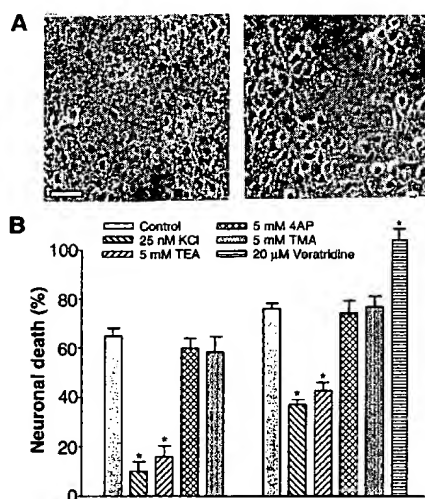


Fig. 4. Protective effects of TEA and 25 mM K^+ were not dependent on an increase in $[Ca^{2+}]_i$. (A) HVA Ca^{2+} currents, activated by a voltage step from -70 to +10 mV, were blocked completely by bath-added 2 μ M gadolinium (Gd^{3+}). The same results were obtained from three additional experiments. (B) Before break, bath application of 5 mM TEA (■) triggered an initial sharp increase in $[Ca^{2+}]_i$, as measured by fura-2 video microscopy, followed by relaxation to a lower plateau value (mean \pm SD; n > 30 neurons for each time point). Results were similar in two additional experiments. TEA plus staurosporine produced a pattern of $[Ca^{2+}]_i$ increase similar to that produced by TEA alone; exposure to 0.1 μ M staurosporine alone for 2 hours did not alter baseline neuronal $[Ca^{2+}]_i$ (data not shown). Gd^{3+} (5 μ M) completely blocked the TEA-induced increase in $[Ca^{2+}]_i$ in the presence of 0.1 μ M staurosporine. After break, in the presence of TEA plus Gd^{3+} (▲), $[Ca^{2+}]_i$ remained at resting levels for up to 16 hours (mean \pm SD; n \geq 200 cells from four experiments). Similarly, 2 μ M Gd^{3+} completely prevented the 25 mM K^+ -induced $[Ca^{2+}]_i$ increase (data not shown). ●, wash control. (C) Ability of 5 mM TEA or 25 mM K^+ to reduce neuronal apoptosis induced by serum deprivation (SD) (left) or staurosporine exposure (STP) (right) was not blocked by coapplication of 2 or 10 μ M Gd^{3+} (n = 20 to 32 cultures per condition except n = 4 for staurosporine plus Gd^{3+} condition). SW, sham wash. (D) Neuroprotective effects of 5 mM TEA or 25 mM K^+ against apoptosis induced by either serum deprivation SD (left) or staurosporine STP (right) were not affected by coapplication of 5 μ M nifedipine (n = 12 for serum deprivation and n = 4 for staurosporine experiments). Cell death was measured as described in Fig. 3. Asterisk indicates significant difference from control at P < 0.05 by t -test with Bonferroni correction for two or three comparisons.

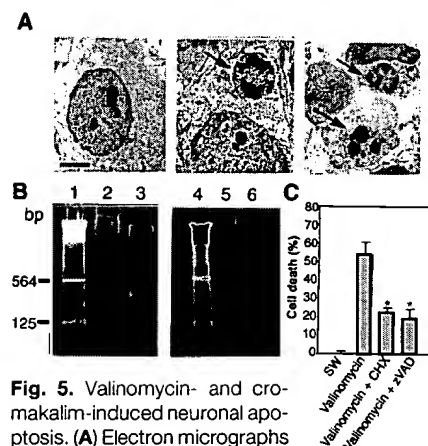
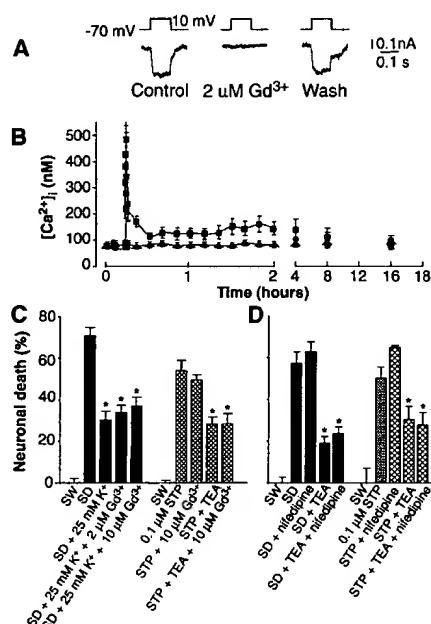


Fig. 5. Valinomycin- and cromakalim-induced neuronal apoptosis. (A) Electron micrographs of a control neuron (left) and apoptotic neurons (arrows) induced by 24 hours of exposure to the selective K^+ ionophore valinomycin (20 nM) (middle) or by the K^+ -channel opener cromakalim (500 μ M) (right). Bar = 3 μ m. (B) DNA laddering on agarose gels after 24 hours of exposure to valinomycin (lane 3) or cromakalim (lane 6). The marker columns (lanes 1 and 4) show Hind III-digested λ DNA. Lanes 2 and 5, controls. (C) Valinomycin-induced neuronal death, assayed by staining with 0.4% trypan blue dye, was attenuated by addition of cycloheximide (1 μ g/ml) (CHX; n = 12) or 100 μ M zVAD (n = 12). Asterisk indicates significant difference from control at P < 0.05 by t -test with Bonferroni correction for two comparisons. SW, sham wash.

ptosis (26). Additional study is needed to delineate the exact mechanisms by which activation of I_K might promote neuronal apoptosis. One possible arena for linkage between these events is in cell cycle control, because K^+ channels and a decrease in intracellular K^+ have been implicated in initiation of mitosis (27), and apoptosis has been postulated to reflect an "abortive mitosis" (28). Furthermore, agents that reduce intracellular K^+ may activate caspases in macrophages or monocytes (29). We suggest that interventions directed at blocking excessive K^+ efflux, in particular by the noninactivating delayed rectifier K^+ channel, be explored as a strategy for attenuating neuronal apoptosis in disease states.

REFERENCES AND NOTES

- M. C. Raff et al., *Science* **262**, 695 (1993); C. B. Thompson, *ibid.* **267**, 1456 (1995); D. W. Choi, *Curr. Opin. Neurobiol.* **6**, 667 (1996).
- B. S. Scott and K. C. Fisher, *Exp. Neurol.* **27**, 16 (1970); M. R. Bennett and W. White, *Brain Res.* **173**, 549 (1979); A. Chazalonis and G. D. Fischbach, *Dev. Biol.* **78**, 173 (1980); F. Collins, M. F. Schmidt, P. B. Guthrie, S. B. Kater, *J. Neurosci.* **11**, 2582 (1991).
- V. Gallo, A. Kingsbury, R. Balázs, O. S. Jorgensen, *J. Neurosci.* **7**, 2203 (1987); J. L. Franklin and E. M. Johnson Jr., *Trends Neurosci.* **15**, 501 (1992); Y. Enokido and H. Hatanaka, *Neuroscience* **57**, 965 (1993); J.-Y. Koh et al., *Exp. Neurol.* **135**, 153 (1995); A. de Luca, M. Weller, A. Fontana, *J. Neurosci.* **16**, 4174 (1996).
- T. Koike, D. P. Martin, E. M. Johnson Jr., *Proc. Natl. Acad. Sci. U.S.A.* **86**, 6421 (1989); E. M. Johnson Jr., T. Koike, J. Franklin, *Exp. Neurol.* **115**, 163 (1992); J. L. Franklin, C. Sanz-Rodriguez, A. Juhasz, T. L. Deckwerth, E. M. Johnson Jr., *J. Neurosci.* **15**, 643 (1995).
- C. Galli, *J. Neurosci.* **15**, 1172 (1995).
- P. A. Lampe, E. B. Combrooks, A. Juhasz, E. M. Johnson Jr., J. L. Franklin, *J. Neurobiol.* **26**, 205 (1995).
- N. Takei and Y. Endo, *Brain Res.* **652**, 65 (1994); D. J. McConkey and S. Orenius, *J. Leukocyte Biol.* **59**, 775 (1996).
- R. D. Murrell and A. M. Tolkovsky, *Eur. J. Neurosci.* **5**, 1261 (1993).
- K. Rose, M. P. Goldberg, D. W. Choi, in *Methods in Toxicology*, C. A. Tyson and J. M. Frazier, Eds. (Academic Press, San Diego, CA, 1993), pp. 46–60.
- J.-Y. Koh, B. J. Gwag, D. Lobner, D. W. Choi, *Science* **268**, 573 (1995).
- Whole-cell voltage clamp was performed on cortical cultures of DIV 7 to 17 in 35-mm culture dishes on the stage of an inverted microscope (Nikon, Japan) with an EPC-7 amplifier (List-Electronic, Germany). The extracellular solution contained 115 mM NaCl, 2.5 mM KCl, 2.0 mM $MgCl_2$, 10 mM Hepes, 0.1 mM 1,2-bis(2-aminophenoxy)ethane- N,N,N',N' -tetraacetic acid (BAPTA), 10 mM D-glucose, and 0.1 μ M tetrodotoxin (TTX). The electrode solution contained 120 mM KCl, 1.5 mM $MgCl_2$, 1.0 mM $CaCl_2$, 2.0 mM Na_2ATP , 1.0 mM BAPTA, and 10 mM Hepes. For HVA Ca^{2+} current recording, the external solution contained 120 mM NaCl, 5 mM $CaCl_2$, 2 mM $MgCl_2$, 10 mM Hepes, 10 mM TEA, 0.0005 mM TTX, and 10 mM glucose. The electrode solution for HVA Ca^{2+} currents contained 130 mM CsCl, 3 mM $MgCl_2$, 10 mM Hepes, 2.5 mM BAPTA, and 5 mM Na_2ATP . Experiments were performed at room temperature (21° to 22°C) and pH 7.3.
- P. R. Adams and M. Galvan, *Adv. Neurol.* **44**, 137 (1986).
- B. Hille, *J. Gen. Physiol.* **50**, 1287 (1967); E. Neher and H. D. Lux, *Physiol. Rev.* **336**, 87 (1972).
- For K^+ measurement, pure neuronal cultures were washed with K^+ -free solution, and cell membranes were disrupted with 0.1% Triton X-100; the extract from eight cultures was pooled for each K^+ measurement (performed with a K^+ -sensitive electrode). Even 9 hours after the onset of serum deprivation, intracellular lactate dehydrogenase and total protein content remained normal, which is an argument against nonspecific membrane leakage or cell death.
- J. W. McDonald, M. I. Behrens, C. Chung, T. Bhat-tacharyya, D. W. Choi, *Brain Res.*, in press.
- Apoptosis was detected by DNA fragmentation (10) and cellular alterations. For electron microscopy, cultures were fixed and then embedded. Sections were cut and stained with lead citrate and uranyl acetate. Cells were examined and photographed with a JEOL 100 CS electron microscope. Tested by applying cycloheximide, phorbol 12-myristate 13-acetate, or BDNF, or re-adding serum, the commitment point for most neurons to die was ≥ 10 hours after apoptotic insults (M. I. Behrens, C. Csemansky, Dugan, D. W. Choi, unpublished data).
- D. Y. Sanchez and A. L. Blatz, *J. Gen. Physiol.* **100**, 217 (1992).
- For fura-2 fluorescence video microscopy, cultures of DIV 12 to 17 were exposed to 5 μ M fura-2/AM plus 0.1% pluronic F-127 for 30 min at room temperature on the stage of a Nikon Diaphot inverted microscope. Fura-2 (excitation: 340, 380 nm; emission: 510 nm) ratio images were acquired with a charge-coupled device camera (Quantex) and digitized (256 \times 512 pixels) by using a Metafluor 2.5 system (Universal Imaging, West Chester, PA). Background fluorescence was subtracted. Calibrated values were obtained in situ by determining F_{min} (2 mM EGTA in Ca^{2+} free-solution) and F_{max} (10 μ M ionomycin in 10 mM Ca^{2+} solution). A K_d of 225 nM was used in the ratio method formula.
- B. C. Pressman, *Annu. Rev. Biochem.* **45**, 501 (1976).
- N. L. Albritton, C. R. Verret, R. C. Wolley, H. N. Eisen, *J. Exp. Med.* **167**, 514 (1988); D. M. Ojcius, A. Zychlinsky, L. M. Zheng, J. D.-E. Young, *Exp. Cell Res.* **197**, 43 (1991); C. L. P. Deckers, A. B. Lyons, K. Samuel, A. Sanderson, A. H. Maddy, *ibid.* **208**, 362 (1993); R. C. Duke, R. Z. Witter, P. B. Nash, J. D.-E. Young, D. M. Ojcius, *FASEB J.* **8**, 237 (1994).
- D. M. T. Politi, S. Suzuki, M. A. Rogawski, *Eur. J. Pharmacol.* **168**, 7 (1989).
- C. Deusch, *Prog. Clin. Biol. Res.* **334**, 251 (1990); B. Rouzaire-Dubois and J.-M. Dubois, *Cell Signal* **3**, 333 (1991).
- S. C. Lee, D. E. Sabath, C. Deusch, M. B. Prystowsky, *J. Cell Biol.* **102**, 1200 (1986); T. Konishi, *J. Physiol. (London)* **411**, 115 (1989).
- R. Reddy et al., *J. Biol. Chem.* **270**, 14340 (1995).
- G. Barbiero, F. Duranti, G. Bonelli, J. S. Amenta, F. M. Baccino, *Exp. Cell Res.* **217**, 410 (1995).
- F. Beauvais, L. Michel, L. Dubertret, *J. Leukocyte Biol.* **57**, 851 (1995).
- C. D. Cone Jr. and C. M. Cone, *Science* **192**, 155 (1976); T. E. DeCoursey, K. G. Chandy, S. Gupta, M. D. Cahalan, *Nature* **307**, 465 (1984).
- D. S. Ucker, *New Biol.* **3**, 103 (1991); G. Ferrari and L. A. Greene, *EMBO J.* **13**, 5922 (1994); N. Heintz, *Trends Biochem. Sci.* **18**, 157 (1993); L. L. Rubin, K. L. Philpott, S. F. Brooks, *Curr. Biol.* **3**, 391 (1993); G. Kroemer, P. Petit, N. Zamzami, J.-L. Vayssière, B. Mignotte, *FASEB J.* **9**, 1277 (1995).
- D. Perregaux and C. A. Gabel, *J. Biol. Chem.* **269**, 15195 (1994); I. Walev, K. Reske, M. Palmer, A. Valeva, S. Bhakdi, *EMBO J.* **14**, 1607 (1995).
- J.-Y. Koh and D. W. Choi, *J. Neurosci. Methods* **20**, 83 (1987).
- This work was supported by NIH grant 30337 (D.W.C.).

2 July 1997; accepted 21 July 1997

Immunotherapy of Tumors with Autologous Tumor-Derived Heat Shock Protein Preparations

Yasuaki Tamura,* Ping Peng,* Kang Liu, Maria Daou, Pramod K. Srivastava†

Immunotherapy of mice with preexisting cancers with heat shock protein preparations derived from autologous cancer resulted in retarded progression of the primary cancer, a reduced metastatic load, and prolongation of life-span. Treatment with heat shock protein preparations derived from cancers other than the autologous cancer did not provide significant protection. Spontaneous cancers (lung cancer and melanoma), chemically induced cancers (fibrosarcoma and colon carcinoma), and an ultraviolet radiation-induced spindle cell carcinoma were tested, and the results support the efficacy of autologous cancer-derived heat shock protein-peptide complexes in immunotherapy of cancers without the need to identify specific tumor antigenic epitopes.

Heat shock proteins (HSPs) GP96, HSP90, and HSP70, when purified from cells, are associated with a broad range of peptides derived from that particular cell, such that the HSPs chaperone the antigenic repertoire of the cells from which they are purified (1). Immunization with HSP-peptide complexes, whether derived endogenously (2–4) or reconstituted in vitro (5, 6), elicits potent T

cell responses against the chaperoned peptides and hence against the cells from which the HSPs are purified, as seen in studies with cancers (1, 3, 7–9), viruses (4, 10–12), model antigens (5, 6, 13), and minor histocompatibility antigens (13). We now examine the use of HSP-peptide complexes in the treatment of a variety of established cancers of spontaneous and experimental origin.

The 3LL (Lewis lung) carcinoma of C57BL/6 mice (14, 15) is a nonimmunogenic spontaneous cancer. It metastasizes naturally to the lungs if injected subcutaneously or in the footpad. HSP GP96 prepa-

Center for Immunotherapy of Cancer and Infectious Diseases, MC1601, University of Connecticut School of Medicine, Farmington, CT 06030, USA.

*These authors contributed equally to this work.

†To whom correspondence should be addressed.

K⁺-dependent Cerebellar Granule Neuron Apoptosis

ROLE OF TASK LEAK K⁺ CHANNELS*

Received for publication, March 14, 2003, and in revised form, May 27, 2003
Published, JBC Papers in Press, June 3, 2003, DOI 10.1074/jbc.M302631200

Inger Lauritzen, Marc Zanzouri, Eric Honoré, Fabrice Duprat, Markus U. Ehrenguber‡, Michel Lazdunski, and Amanda J. Patel§

From the Institut de Pharmacologie Moléculaire et Cellulaire, CNRS, Institut Paul Hamel, 660 route des Lucioles, Sophia Antipolis, 06560 Valbonne, France and the ‡Brain Research Institute, University of Zurich, Winterthurerstrasse 190, CH-8057 Zurich, Switzerland

Rat mature cerebellar granule, unlike hippocampal neurons, die by apoptosis when cultured in a medium containing a physiological concentration of K⁺ but survive under high external K⁺ concentrations. Cell death in physiological K⁺ parallels the developmental expression of the TASK-1 and TASK-3 subunits that encode the pH-sensitive standing outward K⁺ current IK_{so}. Genetic transfer of the TASK subunits in hippocampal neurons, lacking IK_{so}, induces cell death, while their genetic inactivation protects cerebellar granule neurons. Neuronal death of cultured rat granule neurons is also prevented by conditions that specifically reduce K⁺ efflux through the TASK-3 channels such as extracellular acidosis and ruthenium red. TASK leak K⁺ channels thus play an important role in K⁺-dependent apoptosis of cerebellar granule neurons in culture.

Cell excitability is a critical determinant of neuronal survival during brain development (1, 2). K⁺ channels set both the resting membrane potential and the action potential duration. Opening of K⁺ channels and consequent efflux of K⁺ significantly influence neuronal death/survival (3–10). K⁺ channels can either induce neuronal apoptotic cell death (3–7) or, by contrast, protect neurons from ischemia and excitotoxicity (8–10). For instance, overexpression of the weak inward rectifier K⁺ channel ROMK1, causes chronic silencing and apoptosis of rat hippocampal neurons (7), while opening of the K_{ATP} channel with cromakalim is involved in preconditioning and is thus neuroprotective (8, 9). K⁺ channels can also have an oncogenic potential as described for the EAG, HERG, and the KCNK9 (TASK-3) channels (11–14). Thus, depending on the channel subunit and/or the cell type, K⁺ channels can exert either protective or deleterious effects.

Programmed cell death is particularly important in the developing cerebellum (15–17). During the first post-natal week, intense proliferation of the external granular layer (EGL) gives rise to several millions of granule neurons (GN)¹ that migrate

across the molecular and Purkinje layers to reach the inner granular layer (IGL) (15, 17). Massive apoptosis contributes to numerically match GN with the post-synaptic Purkinje neurons. Both synapse-dependent and -independent events are involved in developmental GN apoptosis (15, 17). Various neurons including rat GN die by apoptosis when cultured in a medium containing a physiological concentration of K⁺ (5, 6, 16, 18–20). K⁺-rich depolarizing culture medium as well as K⁺ channel blockers promote neuronal survival *in vitro* (5, 6, 16, 18–24). In the present report, we investigated whether K⁺ channels might be involved in *in vitro* K⁺-dependent granule neuronal apoptosis.

A novel family of mammalian K⁺ channel subunits which comprise four transmembrane segments and two P domains in tandem has recently been discovered (25–28). So far, 15 human 2P domain K⁺ channel subunits have been identified. These subunits dimerize to form functional K⁺ channels (29, 30). The TASK 2P domain K⁺ channels are characterized by a typical leak or background activity and are open at rest. By contrast, the TREK/TRAAK 2P domain K⁺ channels require either a physical (stretch, heat, intracellular acidosis) or chemical (polyunsaturated fatty acids, lysophospholipids, inhalational anesthetics, riluzole, membrane crenators) stimulation to open (25, 26). The 2P domain K⁺ channels are resistant to the classical K⁺ channel blockers including tetraethylammonium (TEA) and 4-aminopyridine (4-AP) (25, 26). TASK-1 and TASK-3 channels (KCNK3 and KCNK9) are reversibly inhibited by extracellular acidosis with a pK value of about 7.3 and 6.7, respectively (30–36). TASK-1 is preferentially inhibited by anandamide, independently of the CB receptor (37), while TASK-3 is blocked by ruthenium red in the micromolar range (38). The TASK channels are additionally down-modulated by the activation of Gq-coupled receptors including the m3 muscarinic receptor (39–41). TASK channels have recently been implicated in central and peripheral chemoreception, in the control of aldosterone secretion from adrenal glomerulosa cells, in cardiac arrhythmias and in general anesthesia (35, 39, 40, 42–45).

TASK-1 and TASK-3 subunits are abundantly expressed in cerebellar GN (31–34, 36, 41, 46, 47). Rat GN express high levels of an outwardly rectifying K⁺ current, termed IK_{so} (standing outward K⁺ current), which shares all the biophysical, pharmacological, and regulation characteristics of the TASK-1 and TASK-3 two-pore domain K⁺ channels (41, 48, 49). In this study, we demonstrate that TASK-3 channels contribute to IK_{so} and are involved in K⁺-dependent rat granule neuronal death in culture.

* This work was supported by the Swiss National Science Foundation (Grant no. 31-57125.99 (to M. U. E.)) and the CNRS and the Institut Paul Hamel. The costs of publication of this article were defrayed in part by the payment of page charges. This article must therefore be hereby marked "advertisement" in accordance with 18 U.S.C. Section 1734 solely to indicate this fact.

§ To whom correspondence should be addressed. Tel.: 33-4-93-95-77-02/03; Fax: 33-4-93-95-77-04; E-mail: ipmc@ipmc.cnrs.fr.

¹ The abbreviations used are: GN, granule neurons; EMEM, Eagle's basal medium; PI, propidium iodide; DAPI, 4',6-diamidino-2-phenylindole; EGFP, enhanced green fluorescent protein; WT, wild type; DIV, days *in vitro*; 4-DAMP, 4-diphenylacetoxyl-N-methylpiperidine methiodide; TUNEL, terminal deoxynucleotidyltransferase-

mediated dUTP nick end-labeling; SFV, Semliki Forest Virus; TEA, tetraethylammonium.

MATERIALS AND METHODS

Neuronal Cell Cultures—Cerebellar granule cells were prepared from 7–8-day-old Wistar rats (Iffa Credo, France). Neurons were seeded on poly-L-lysine (50 μ g/ml)-coated dishes or coverslips at a density of 2.5×10^6 cells/cm² and cultured in Eagle's basal medium (EMEM, Sigma) supplemented with 10% fetal calf serum (Invitrogen), 25 mM KCl, 0.5% penicillin-streptomycin. To prevent growth of glial cells, cytosine arabinoside (Ara-C) (10 μ M) was added to the cultures 24 h following plating. GN were similarly prepared from 5–6-day-old OF1 mice.

Hippocampal neurons were prepared from 18–19-day fetal Wistar rats (Iffa Credo, France). Neurons were seeded on poly-D-lysine-coated plates at a density of 2×10^6 cells/cm² and cultured in EMEM supplemented with 10% horse serum (Sigma) and 0.5% penicillin-streptomycin. After 48 h, the serum-supplemented medium was replaced by EMEM containing B27 supplement, and cells were used for viral infection experiments after 1 week.

Electrophysiological Recordings—The electrophysiological procedure has been previously described in detail elsewhere (31, 37, 44). Whole cell currents were recorded in the perforated configuration with amphotericin B (240 μ g/ml). The standard external solution contained 120 mM NaCl, 5 mM KCl, 2 mM MgCl₂, 0.5 mM CaCl₂, 5 mM glucose, 10 mM HEPES pH 7.4 with NaOH. The pipette solution contained 125 mM KCl, 5 mM MgCl₂, 0.1 mM EGTA, and 5 mM HEPES pH 7.2 with KOH. Cells were continuously superfused with a microperfusion system during the time course of the experiments (0.1 ml/min). Experiments were performed at room temperature. The K⁺-rich solution contained 120 mM KCl instead of NaCl. pH of the external solution was adjusted with HCl. Staurosporine (Sigma) stock solution was made in Me₂SO at a concentration of 10 mM. Methanandamide was provided as an ethanol solution (BioMol). VDM11 (a gift of V. Di Marzo) and AOCF₃ (BioMol) were dissolved in ethanol at a concentration of 100 mM. Muscarine (Sigma) stock solution was made in water at a concentration of 100 mM. 4-Di-phenylacetoxyl-N-methylpiperidine methiodide (4-DAMP) (RBI), tetraethylammonium (TEA, Sigma), 4-aminopyridine (4-AP), and ruthenium red (Sigma) were directly dissolved in the external medium. Solvents were routinely included in the control solutions when needed, and pH was always carefully adjusted.

Induction of Apoptosis—Unless otherwise stated, the GN were maintained for the first 8 days *in vitro* (8 DIV) in a standard medium (S⁺, 25K) (EMEM, Sigma) containing 10 μ M cytosine arabinoside. Hereafter, the cells were washed once and then switched to a serum-free medium containing 5 mM K⁺ and 20 mM NaCl instead of KCl (S⁻, 5K). Sister cultures were washed identically and maintained in serum-free medium containing 25 mM KCl (S⁻, 25K). In control experiments, the effect of short term serum deprivation was determined on cell survival. Hydrolyzed fetal calf serum (Invitrogen) was used in the S⁺ conditions, because addition of fresh normal calf serum is known to be toxic to mature GN (50, 51). During a 15-h treatment (maximal time window used in the present report), serum deprivation did not significantly alter cell survival in either 5 mM or 25 mM KCl-treated cultures. Both the S⁻ 5 K and 25 K media lacked cytosine arabinoside that has been previously shown to be toxic to cerebellar granules after K⁺ withdrawal (51). In this model of culture, neuronal death is thus mainly due to K⁺ withdrawal (51). In the complete absence of cytosine arabinoside in the culture medium, both glial cells and GN survive up to 10 days in the S⁺, 25K medium, whereas only glial cells survive in the S⁻, 5K medium. Cell death in the 5K medium was therefore independent of the presence or the absence of cytosine arabinoside, *i.e.* of glial cells. pH was buffered using either: 1/increasing concentrations of HCO₃⁻ in the EMEM/osmotic compensation with NaCl; 2/HEPES 10 mM titrated with NaOH (2 M in EMEM). Osmolarity of the culture medium was checked with a Knauer automatic osmometer. In experiments with pharmacological agents, solvents were always included in the control solutions when needed.

Assessment of Cell Death—Neuronal injury was quantitatively assessed by the measurements of lactate dehydrogenase (LDH) release in the medium or by staining the nuclei with the chromatin-fixing dyes propidium iodide (PI) or 4',6'-diamidino-2-phenylindole (DAPI). For staining purposes, cells were fixed with freshly prepared paraformaldehyde (PFA) 4%. For nuclear staining with PI, cells were permeabilized with 70% ethanol and incubated in phosphate-buffered saline containing propidium iodide (5 μ g/ml during 10 min). The nuclei of dying cells were highly fluorescent and condensed compared with live cells. Neuronal cell death was scored by counting in at least 6 randomly chosen subfields with a 25 \times objective for each sample. Results are mean \pm S.E. of counting in three independent experiments. Staining

with DAPI was performed using a ready-to-use mounting medium containing DAPI (Vectashield, Vector). Further assessment of apoptosis was performed as described below.

RNA Extraction and Reverse Transcription PCR—Cells grown in (S⁺, 25K) in 60-mm dishes were recovered for RNA analysis at distinct days *in vitro* (DIV 1, 3, 5, and 8). For comparison, cerebellum was isolated from 7-, 10-, 14-, and 21-day-old rats. Total RNAs were extracted by the TRIzol method (Invitrogen) for cerebellum and by the RNeasy Mini Kit (Qiagen) for cultured granule neurons. Reverse transcription was performed with 2 μ g of total mRNA, treated for 30 min with DNaseI (Roche Applied Science), and reverse-transcribed with Superscript II reverse transcriptase (Invitrogen). Real-time PCR analysis (SYBR Green Mastermix Plus, Eurogentec) was performed to estimate the level of expression of both TASK-1 and TASK-3 in cerebellum and cultured granule neurons. Real-time PCR assays for each gene target were performed on cDNA samples in 96-well optical plates on an ABI Prism 7700 Sequence Detection system (PE Biosystems). PCR data was captured using Sequence Detector Software. The data were analyzed using the comparative C_T method where the amount of target is normalized to an endogenous reference (cyclophilin D) (User Bulletin N°2 Applied Biosystems). Experiments were performed in triplicate. The following primers were used for PCR: rTASK-1, for: 5'-CGGCTCCGCAACGTC-TAT-3' and rev: 5'-TTGTACCAGAGGCACGAGCA-3'; rTASK-3, for: 5'-GACGTGCTGAGGAACACCTACTT-3' and rev: 5'-GTGTGCATTC-CAGGAGGGA-3'; cyclophilin D, for: 5'-GGCTCTTGAATGGAC-CCTTC-3' and rev: 5'-CAGCCAATGCTTGATCATATTCTT-3'. Standard curves were generated for each set of primers using serial dilutions of rat brain cDNA to ensure a similar efficiency of amplification.

DNA Fragmentation Analysis—Cells (60-mm culture plates) were lysed in extraction buffer (5 mM Tris, pH 7.5, 100 mM EDTA, 1% sodium dodecyl sulfate (SDS), and 200 μ g/ml proteinase K) at 37 °C overnight. DNA was subsequently extracted with phenol and chloroform/isoamyl alcohol and treated with RNase A (50 μ g/ml) at 37 °C for 1 h. DNA was precipitated with isopropyl alcohol and analyzed on an agarose gel (1.2% agarose (SeaKem GTG, FMC BioProducts)). The gel was stained with ethidium bromide and visualized using a UV light source. For terminal deoxynucleotidyl transferase-mediated DNA nick-end labeling (TUNEL) labeling, the *in situ* cell death detection kit (fluorescein) from Roche Applied Science was used according to the manufacturer's instructions.

Assessment of Caspase Activity—After incubation of GN in low K⁺ media for 4 h (at distinct pH: 6.4, 6.8, and 7.2), cells were rinsed in phosphate-buffered saline, gently scraped, pelleted by centrifugation, and resuspended in 40 μ l of lysis buffer, and caspase activity was determined using the Neosystem kit. Results are the mean \pm S.E. of triplicate values.

Generation of Semliki Forest Virus (SFV) Vectors—The mutant vector SFV(PD) carries two point mutations in the non-structural protein 2 gene (S259P and R650D) and is characterized by a lack of cellular toxicity and an increased level of transgene expression, as compared with the wild-type SFV vector. To express the EGFP reporter gene (Clontech) separately from any gene of interest, we transformed pSFV(PD) into a double-subgenomic RNA promoter vector, termed pSFV(PD)-Sub-GFP. Briefly, using pSFV-GFP as a template, we amplified by PCR the cDNA encompassing the 26 S subgenomic RNA promoter region (including the 19 nucleotides upstream from the 26 S subgenomic RNA), and the EGFP gene with primers containing a *NotI* and an *ApaI* site (forward and reverse primer, respectively). The resulting PCR fragment was then inserted into the *NotI/ApaI* sites of pSFV(PD), yielding pSFV(PD)-Sub-GFP. This vector retains in the multiple cloning site the following unique restriction sites to insert genes of interest under the control of the first 26 S subgenomic RNA promoter: *RsrII-BssHII-XmaI-SmaI-XhoI-SpeI-NotI* (5' to 3'-end). We used pSFV(PD)-Sub-GFP to insert the following cDNAs: mTREK-1, mTREK1^{E306A}, rTASK-1, rTASK-3, rTASK-1^{G95E}, and rTASK-3^{G95E}. *In vitro* transcribed vector RNA was introduced with RNA from pSFV-Helper2 into baby hamster kidney 21 (BHK) cells by electroporation. Recombinant SFV particles were harvested after 24 h, activated with α -chymotrypsin, centrifuged at 35,000 rpm for 2 h, and resuspended in neuronal medium. TASK-1 and TASK-3 viruses were generated in a culture medium containing 25 mM KCl.

TASK Viral Overexpression in Cerebellar Granule and Hippocampal Neurons—Hippocampal neurons 6 DIV were infected as indicated above, but the media were replaced by freshly pH-adjusted EMEM after 2 h of incubation. After 16–24 h, cells were rinsed and fixed in 4% paraformaldehyde and used for DAPI and TUNEL staining. For TUNEL labeling we used the *in situ* detection kit (TMR-red) from Roche Applied Science. Cells were analyzed by fluorescence microscopy. Chan-

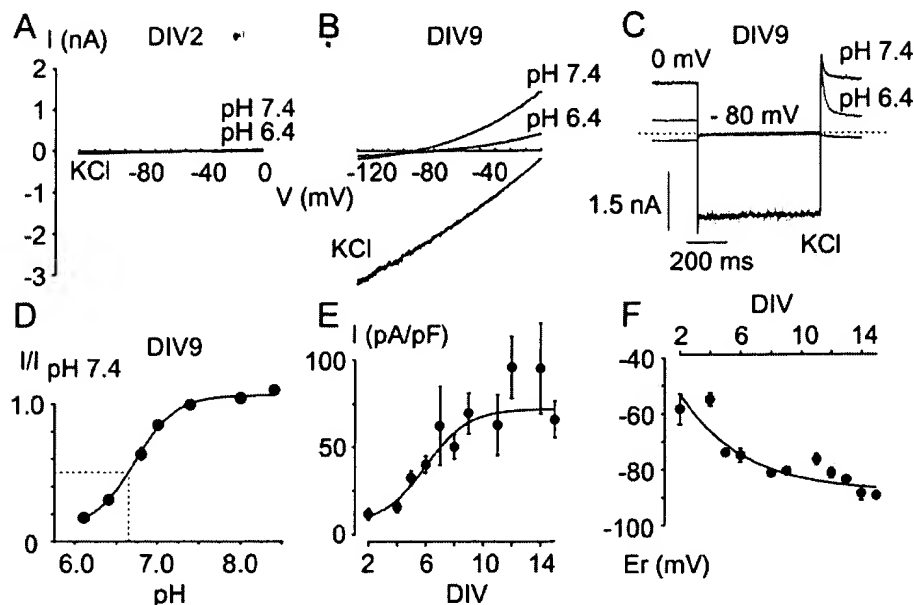


FIG. 1. Developmental expression of IK_{so} in cultured rat cerebellar granule neurons. *A*, I-V curve of a DIV 2 GN recorded with the whole cell amphotericin B perforated patch clamp technique. The cell was held at a holding potential of 0 mV and voltage ramps of 500 ms in duration were applied every 10 s to -120 mV. Current was recorded under low K^+ condition containing 5 mM KCl at pH 7.4 and 6.4. IK_{so} was finally recorded in the K^+ -rich medium containing 125 mM KCl. *B*, same as *A* with a 9 DIV GN. IK_{so} was recorded in the presence of 10 mM TEA and 3 mM 4-AP. *C*, recording of IK_{so} with a voltage step from a holding potential of 0 mV to -80 mV; same cell as in *B*. *D*, gradual inhibition of IK_{so} , normalized to the value recorded at pH 7.4, at decreasing external pH. This dose effect curve was constructed in the presence of 10 mM TEA and 3 mM 4-AP at a holding potential of 0 mV. A pK value of 6.7 was estimated by fitting the experimental data point with a Boltzmann relationship. Each data point is the mean of 3–16 cells. *E*, relationship between IK_{so} current density measured at 0 mV as a function of the duration of GN culture (DIV). Each data point is the mean of 3–15 cells. *F*, evolution of the resting membrane potential during development of cultured GN (DIV). Each data point is the mean of 3–11 cells.

nel-expressing cells were visualized by green fluorescence, TUNEL-labeled cells by red fluorescence, and DAPI-colored nuclei were visualized by blue fluorescence. Apoptotic cells were scored by counting 80 green cells from each culture dish, two dishes per condition. The results were pooled from four separate experiments. In each case, cell viability/death were estimated by both DAPI and TUNEL labeling. 5 DIV GN cultures were infected by addition of virus into the culture medium. The viruses were left for 36 h, because of a weaker efficiency of infection compared with hippocampal neurons, then GN were transferred to virus-free media containing 5 mM KCl. Cells were fixed with paraformaldehyde after 6 h. After fixation, cells were mounted in DAPI-containing mounting medium, and the number of dead (pyknotic or fragmented nuclei) or alive green fluorescent cells were counted by fluorescence microscopy. Non-neuronal cells, which were bigger and less bright after the DAPI staining were not counted. The results were pooled from four separate experiments.

RESULTS

Developmental Expression of IK_{so} and TASK Channel Subunits in Rat Cerebellar Granule Neurons— IK_{so} was present at a very modest level in young neurons (DIV 1–3), whereas there was a gradual and substantial increase in its amplitude in older cultures (Fig. 1, *A–E*). The current density of IK_{so} and the resting membrane potential reached a maximum at about 9–10 DIV (Fig. 1, *E–F*). IK_{so} displayed a typical background activity, which was inhibited at acidic extracellular pH (Fig. 1, *B–C*). The effect of external acidosis was dose-dependent and half-maximal inhibition was observed at a pH value of 6.7 (Fig. 1*D*). In 9 DIV GN, decreasing external pH to 6.4 mimicked the effect of an increase in external K^+ and induced membrane depolarization (-74.7 ± 0.9 mV; $n = 37$; -57.1 ± 1.6 mV; $n = 26$; -35.9 ± 1.5 mV; $n = 19$ for 5K pH 7.4, 5K pH 6.4, and 25K pH 7.4). IK_{so} was not affected by the K^+ channel blockers TEA (10 mM) and 4-AP (3 mM) (Fig. 1, *B–C*). Real-time PCR analysis revealed that the level of TASK-1 and TASK-3 transcripts gradually increased with time both in culture and *in vivo* (Fig. 2, *A–B*). When compared with the *in vivo* situation, the level of transcripts in culture was higher by about 3–6-fold for TASK-1

and TASK-3, respectively. However, the presence of various cell types in the cerebellum that may lack TASK subunits could have led to an underestimation of TASK-1/3 *in vivo*. Moreover, the ratio between TASK-3 and TASK-1 mRNAs increased from about 0.4 *in vivo* to 1 *in vitro* (Fig. 2, *A–B*).

Developmental Regulation of K^+ -dependent Granule Neuron Death and Acidic Protection—Rat GN were cultured in 25 mM K^+ and then shifted to a medium containing 5 mM K^+ at distinct DIV (Fig. 3). Cell death was estimated at 15 h following the shift to low K^+ by the number of pyknotic/fragmented nuclei visualized with either PI or DAPI staining (Fig. 3, *A–B*). At a physiological pH (7.4), granule neurons at 1–3 DIV survived in low K^+ (5 mM) whereas cultures older than 4 DIV gradually died (Fig. 3, *A–B*). Maximal sensitivity to external K^+ , with about 90% of cell death was reached at 6 DIV (Fig. 3*A*). Similar experiments were performed with the extracellular pH lowered from 7.4 to 6.4 (Fig. 3, *A–B*). In young cultures (1–3 DIV), lowering pH to 6.4 in low K^+ conditions enhanced cell death (Fig. 3*A*). However, GN older than 4 DIV was fully protected from K^+ -dependent cell death by acidic pH (Fig. 3, *A–B*). A similar protective effect of external acidosis was observed in the presence of either HCO_3^- (5% CO_2) or HEPES (air) as a buffer in the culture medium. Next, we monitored lactate dehydrogenase (LDH) release, as an indicator of cell lysis and death, in young (4 DIV) and older (5–8 DIV) GN in low K^+ conditions (15-h treatment) at both pH 7.4 and pH 6.4 (Fig. 3*C*). The release of LDH from 4 DIV neuron was modest and insensitive to external acidosis whereas older GN (5–8 DIV) cultured in low K^+ conditions displayed a substantial pH-sensitive LDH release (Fig. 3*C*). 8 DIV GN cultured in media containing increasing concentrations of external K^+ ranging from 5 to 25 mM K^+ were gradually protected (Fig. 3*D*).

We induced 8 DIV GN death in the 25 mM K^+ -rich medium at pH 7.4 by removing serum (24-h long term treatment) or adding 500 nM staurosporine (Fig. 3*E*). Both experimental ap-

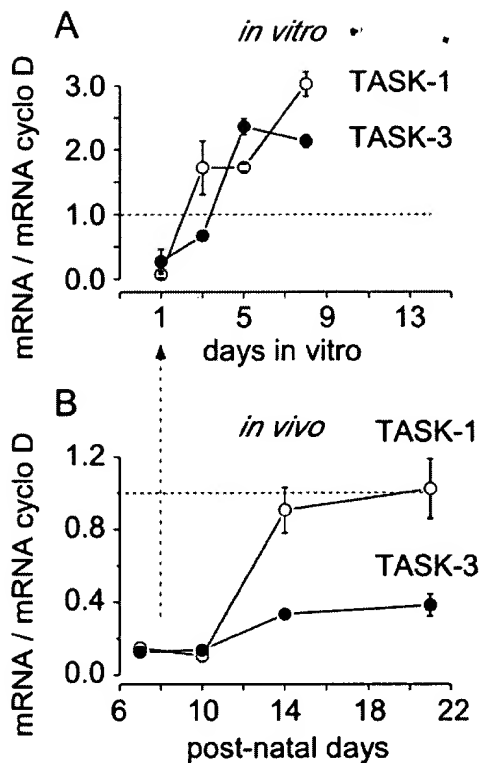


FIG. 2. *In vitro* and *in vivo* cerebellar expression of TASK-1 and TASK-3. **A**, real-time PCR analysis of TASK-1 and TASK-3 expression in cultured rGN. GN were isolated from 7-day-old rat cerebellum and cultured in S^+ 25 mM K^+ . RNAs were extracted from 1-, 3-, 5-, and 8-day-old cultures. **B**, real-time PCR analysis of TASK-1 and TASK-3 expression in rat cerebellum at different postnatal days of development. Expression levels of TASK subunits were normalized to the level of cyclophilin D, which remained constant both *in vitro* and *in vivo* during development. The dashed lines indicate the standard cyclophilin D.

proaches led to a significant increase in cell death although the effect of staurosporine was substantially more dramatic than the effect of serum starvation. In both conditions, cell death was not affected by extracellular acidic pH, although in parallel control experiments acidosis to pH 6.4 fully protected the sister GN culture from K^+ -dependent death (Fig. 3F). These data demonstrate that acidic neuroprotection is thus specific to K^+ -dependent GN death.

pH Sensitivity of Granule Neuron K^+ -dependent Death—8 DIV GN were incubated for 8 h in low K^+ medium at various extracellular pH values ranging from 6.0 to 8.5 in order to determine the pH sensitivity of K^+ -induced GN death (Fig. 4A). At pH values lower than 6.6, K^+ -dependent cell death was completely abolished. Half-maximal death was observed at a pH of about 7.0 (Fig. 4A). As another index of cell apoptosis, DNA fragmentation was observed in 8 DIV neurons cultured in low K^+ condition at pH values higher than 6.6 (Fig. 4B). Again, half-maximal DNA fragmentation was observed at a pH of about 7.0. A protective effect was also observed in the 25 mM K^+ -rich condition at pH 7.4 (Fig. 4B). 8 DIV GN cultured for 15 h in a low K^+ medium at pH 7.4 were TUNEL positive, demonstrating apoptotic cell death (Fig. 4C). Lowering external pH to 6.4 protected GN from cell death and almost completely eliminated the TUNEL signal (Fig. 4C). Caspase activation, a hallmark of apoptosis, was measured using the fluorogenic tetrapeptide substrate Ac-DEVD-MCA. The DEVD-MCA cleavage activity is specific to group II caspases, since it is blocked by the specific inhibitor DEVD-CHO. Cells were recovered at 4 h following transfer to low K^+ medium (Fig. 4D). Very low caspase activity was observed in cell extracts from

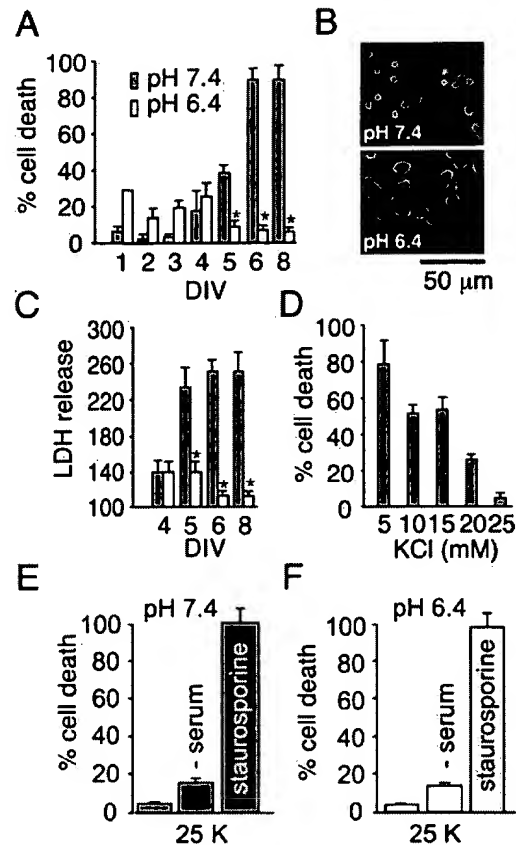


FIG. 3. K^+ -dependent cell death of cultured rat granule neurons and acidic protection. **A**, quantitative analysis of the effect of a low K^+ medium on rGN apoptosis as a function of development (DIV). rGN at different DIV were exposed to 5 mM K^+ for 15 h and analyzed for cell viability by PI labeling. Cells were cultured in 25 mM K^+ and transferred to 5 mM K^+ at both pH 7.4 (dark gray bars) and pH 6.4 (light gray bars) at distinct DIV as indicated. **B**, fluorescence images of 8 DIV cultures illustrating PI-stained cell cultures in 5 mM K^+ condition at both pH 7.4 and 6.4. **C**, release of LDH expressed as the percentage of release of sister cultures maintained in the presence of 25 mM KCl. LDH release was measured at different DIV, as indicated, in the presence of 5 mM KCl for 15 h at either pH 7.4 or 6.4. **D**, quantitative analysis of cell death induced by 8 h long exposure of 8 DIV cultures to different concentrations of K^+ . Cell death was estimated by PI-fluorescence microscopy. After 8 h the cells were fixed, stained by PI, and visualized by fluorescence microscopy. Apoptotic cells were scored by counting at least 600 cells in several randomized subfields for each sample from three different experiments. **E**, effect of long term serum starvation and staurosporine 500 nM treatment for 24 h on GN survival. These experiments were performed in the presence of the depolarizing K^+ -rich solution (containing 25 mM KCl) at pH 7.4. **F**, similar experiments at pH 6.4. Control experiments in sister cultures showed protection against K^+ deprivation-induced apoptosis (5 mM KCl) at pH 6.4 for 6 h (not shown). In these experiments cell viability was quantified by PI staining.

cultures at pH values of 6.4 and 6.8, whereas activity at pH 7.2 was dramatically increased.

Identical Pharmacological and Regulation Properties between IKso/TASK and K^+ -dependent Granule Neuron Death— K^+ -dependent cell death of 8–9 DIV GN, similarly to IKso, was not sensitive to 4-AP (2 mM) and TEA (3 mM) although acidosis to pH 6.4, which inhibits IKso, fully protected these neurons (Fig. 1, B–C, 5C). IKso was not affected by 3 μ M methanandamide (a preferential blocker of TASK-1, Ref. 37) and only partially inhibited by 10 μ M methanandamide ($n = 16$) (Fig. 5A). No protection was observed with 10 μ M methanandamide in the presence or in the absence of the anandamide transporter inhibitor VDM11 and the anandamide amidase inhibitor AACOCF₃ (Fig. 5D). Ruthenium red, a blocker of TASK-3 (52),

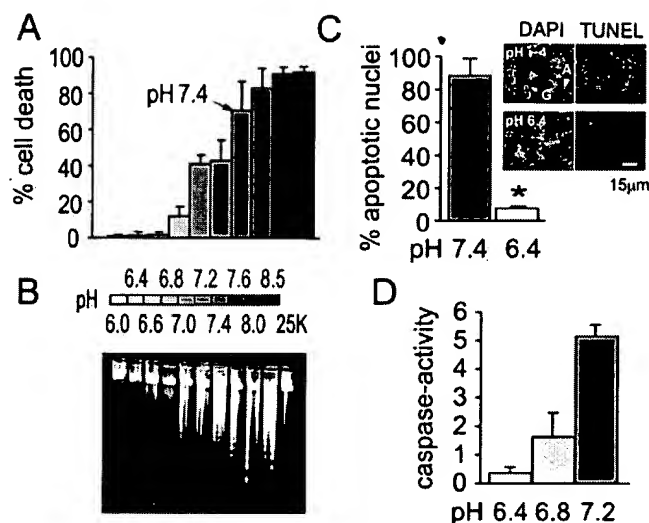


FIG. 4. pH sensitivity of rat granule neuron K^+ -dependent cell death in culture. *A*, quantitative analysis of the effects of external acidosis on K^+ -dependent apoptosis in 8 DIV rGN. Cells were exposed to 5 mM K^+ at pH values between pH 6.0 and 8.5. After 8 h the cells were fixed, stained by PI, and visualized by fluorescence microscopy. Apoptotic cells were scored by counting at least 600 cells in several randomized subfields for each sample from three different experiments. *B*, acidic pH inhibits DNA fragmentation induced in the low K^+ condition. After 8 h of incubation in the medium containing 5 mM KCl, genomic DNA was extracted and visualized by gel analysis. *C*, effect of extracellular acidosis on GN apoptosis (TUNEL labeling). The dark gray bar indicates pH 7.4 and light gray bar pH 6.4. Fluorescence images of 8 DIV cultures after 15 h of K^+ deprivation at both pH 7.4 and 6.4. Cells were stained with DAPI (blue) and TUNEL-labeled (green). Non-neuronal cells, which were bigger and less bright after DAPI staining, were excluded from the counting. *A*, astrocyte, *G*, granule neuron. *D*, inhibition of caspase activation under low K^+ (arbitrary units/h/mg) by acidic pH. After 4 h of incubation in media with 3 distinct pH values, pH 6.4, 6.8, and 7.2, DEVD-MCA cleavage activity in whole cell extracts was determined by measuring the production of fluorescent MCA. Caspase-specific activity was calculated from the linear part of fluorimetry recording and expressed in arbitrary units/h/mg proteins.

dose-dependently inhibited IKso (Fig. 5*B*). At 10 μ M, 100% of the pH 6.4-sensitive component of IKso was inhibited ($n = 3$) (Fig. 5*B*). GN was gradually protected from K^+ withdrawal cell death by increasing concentrations of ruthenium red (Fig. 5*D*). No toxic effect of the polycationic dye was observed on GN maintained in the K^+ -rich solution (Fig. 5*D*, inset).

IKso, as previously reported (41, 48), was reversibly inhibited by muscarinic stimulation (Fig. 6*A*). Muscarine mimicked the effect of extracellular acidosis and induced GN depolarization (Fig. 6*A*, inset). Muscarine also significantly protected GN from K^+ -dependent cell death at pH 7.4 (Fig. 6*B*). This protective effect was reversed by the muscarinic m1/m3 receptor antagonist 4-DAMP (Fig. 6*B*).

Transfer of K^+ - and pH-dependent Cell Death to Hippocampal Neurons by Viral Expression of TASK Subunits—We next investigated whether overexpression of TASK channel subunits in hippocampal neurons that lack IKso, *i.e.* a TASK-like current, and are known to survive in low K^+ conditions (5 mM), could induce a K^+ - and pH-sensitive cell death (Fig. 7). We used a non-cytotoxic Semliki Forest Virus mutant (SFV(PD)) to introduce rTASK channel subunits into cultured neurons (53). Hippocampal neurons (7 DIV) infected with control virus, bearing only EGFP, were highly fluorescent as early as 5-h postinfection. Cells were either fixed at 16–24 h postinfection for cell viability experiments, or tested for channel expression in electrophysiology (Fig. 7). Cells expressing EGFP alone showed normal morphology and displayed electrophysiological properties similar to those of non-infected cells, *i.e.* a lack of IKso (Fig.

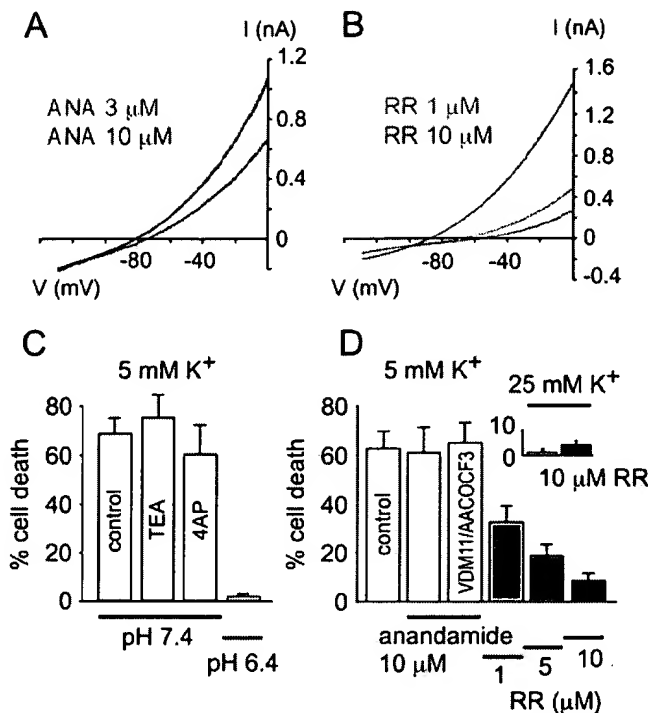


FIG. 5. Pharmacology of rat granule neuron *in vitro* K^+ -dependent cell death. *A*, effect of 3 (light gray) and 10 μ M methanandamide (dark gray) on IKso recorded in a 8 DIV granular neuron. *B*, effect of 1 (light gray) and 10 μ M ruthenium red (dark gray) on IKso recorded in a 8 DIV granular neurons. In *A* and *B*, the holding potential was 0 mV. *C*, effect of TEA and 4AP on low K^+ -induced GN apoptosis at pH 7.4. In these experiments, neurons were treated for 7 h in the low K^+ condition containing 5 mM KCl with 3 mM TEA and 2 mM 4-AP. Acidic pH 6.4, however, produced a significant neuroprotection. Cell death was determined by DAPI staining. *D*, effect of 10 μ M methanandamide, 1, 5, and 10 μ M ruthenium red on low K^+ -induced GN apoptosis at pH 7.4. The effect of 10 μ M methanandamide was also investigated in the presence of 10 μ M VDM11 and 10 μ M AACOCF₃, inhibitors of anandamide transporter and amidase. In these experiments, neurons were treated for 7 h in the low K^+ condition containing 5 mM KCl with the indicated pharmacological agents. In the K^+ -rich medium, 10 μ M ruthenium red did not affect cell viability (inset).

7*A*). DAPI or TUNEL staining revealed no sign of cell death (Fig. 7*E*). In the TASK-infected cells, a pH-sensitive IKso-like current was recorded (Fig. 7, *B–C*). TASK-3 currents were consistently higher than the TASK-1 currents and partially inhibited at pH 6.4 (Fig. 7, *B–C*). Cells infected with rTASK-1/EGFP or rTASK-3/EGFP, only showed a very weak green fluorescence at 16–24-h postinfection when cultured in low K^+ conditions (Fig. 7*D*). DAPI staining revealed a high number of fragmented nuclei that were also TUNEL-positive (Fig. 7, *D–E*). The mechano-gated K^+ channel TREK-1, unlike the constitutively active TASK K^+ channels, did not alter cell survival (Fig. 7*E*). However, expression of the TREK-1 mutant E306A, that is locked in the open conformation (54), similarly to TASK subunits, induced hippocampal neuron death ($82.3 \pm 3.1\%$ apoptotic neurons in 5 mM K^+). The time course of cell death was always faster with TASK-3 in comparison to TASK-1 upon switching to low K^+ conditions. When hippocampal cells expressing TASK-1 or TASK-3 were maintained at pH 6.4 in low K^+ or at pH 7.4 in 25 mM K^+ , cell death was reduced (as visualized by DAPI and TUNEL staining) and strong EGFP fluorescence (showing healthy infected neurons) was observed (Fig. 7, *D–E*). Protection was however consistently weaker with the TASK-3-infected neurons. As previously reported (46), the G95E mutation in the P1 region induced a loss of rTASK-1/3 channel function when expressed in *Xenopus* oocytes (Fig. 8,

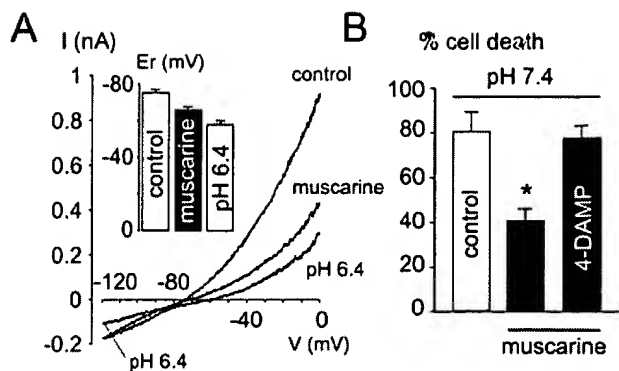


FIG. 6. Muscarinic protection of rat granule neuron K^+ -dependent cell death in culture. *A*, effect of 100 μ M muscarine on IKso recorded in a 8 DIV GN in the presence of 10 mM TEA and 3 mM 4-AP. The cell was held at a holding potential of 0 mV and voltage ramps of 500 ms in duration were applied every 10 s to -120 mV. Current was recorded in the presence of 5 mM KCl at pH 7.4 with or without 100 μ M muscarine and finally at pH 6.4. The inset illustrates the effect of muscarine (100 μ M) and pH 6.4 on GN resting membrane potential in 8 DIV GN. *B*, effect of muscarine 100 μ M in the absence and in the presence of 10 μ M 4-DAMP on GN cell death determined by DAPI staining. Cells were treated for 8 h in low K^+ in the presence or the absence of the indicated agents.

A–B). Hippocampal neurons infected with the rTASK-1^{G95E} or rTASK-3^{G95E} mutants were healthy, displaying a bright green fluorescence, and no sign of cell death was detected in the low K^+ condition at pH 7.4 (Fig. 7E).

Expression of Dominant-negative Loss of Function TASK Mutants Protects Cerebellar Granule Neurons from Low K^+ -induced Cell Death.—The loss of function G95E subunits behaved as dominant-negative mutants, suppressing the activity of their homologous WT channels in a dose-dependent manner, when expressed in *Xenopus* oocytes (Fig. 8, *A–B*). Again, it should be noted that the amplitude of the rTASK-3 currents was much stronger compared with rTASK-1. The concentration of injected rTASK-3 mRNA needed to be diluted at least by 200-fold to record currents of comparable amplitude (Fig. 8, *A–B*). Next, we co-expressed the rTASK-1^{G95E} with WT rTASK-3 and the rTASK-3^{G95E} mutant with WT rTASK-1 (Fig. 8, *C–D*). The G95E mutants reduced the amplitude of the non-homologous WT rTASK current in a dose-dependent manner, thus behaving as trans-dominant-negative mutants (Fig. 8, *C–D*). By contrast, mTREK-1^{G144E} did not affect rTASK-1 ($n = 28$) or rTASK-3 ($n = 27$) currents even with a 100-fold mRNA excess, although it consistently inhibited TREK-1 WT ($n = 28$) (not shown). We took advantage of the rTASK-1/-3^{G95E} dominant-negative mutants to genetically inactivate the endogenous rTASK subunits in cultured GN (Fig. 8E). GN were infected at 6 DIV (in 25 mM K^+) and then transferred to low K^+ after 30 h of culture. The cells were fixed and analyzed for cell viability with DAPI staining after 6 h of culture in low K^+ condition. At this time point, about 50% of the GN had died in either EGFP- or mTREK-1/EGFP-expressing neurons (Fig. 8E). The dominant-negative mutants rTASK-1^{G95E} and rTASK-3^{G95E} significantly reduced the number of dying neurons (Fig. 8E). By contrast, the expression of WT rTASK-1 or rTASK-3 increased cell death to about 100% (Fig. 8E).

The Murine OF1 Cerebellar Granule Neurons Survive in Low K^+ Conditions.—The amplitude of IKso in murine OF1 GN was significantly smaller compared with the one recorded in rat GN cultured under the same conditions (8–9 DIV) (Fig. 9A). Unlike rat, mouse OF1 GN survived upon K^+ withdrawal after 8 h (Fig. 9B).

DISCUSSION

Functional Link between IKso and K^+ -dependent Rat GN Cell Death.—Mature rat GN (8–9 DIV) undergo cell death if cultured in a physiological K^+ concentration of 5 mM. Neuronal death is prevented in a depolarizing medium containing 25 mM K^+ . GN, which are grown in a high K^+ medium, die within a few hours if transferred to a medium containing low K^+ . Young neurons (1–3 DIV), lacking IKso, are resistant to low K^+ -induced cell death. Similarly, rat mature hippocampal neurons and mouse OF1 GN, with a very small IKso, do not undergo K^+ -dependent cell death. Both GN death and IKso are resistant to the K^+ channel blockers TEA and 4-AP. Decreasing extracellular pH inhibits IKso and prevents K^+ -dependent cell death of mature GN as visualized by nuclear condensation. Furthermore, extracellular acidosis abolishes LDH release, DNA fragmentation and caspase activation, hallmarks of apoptotic cell death. Similarly, ruthenium red and muscarinic inhibition of IKso also protect mature GN from K^+ -dependent cell death. All together, these results indicate a correlation between IKso and K^+ -dependent GN cell death in culture.

TASK Channels and Cerebellar Granule Neurons IKso.—IKso, recorded in cultured GN or in cerebellum thin slices, is an outwardly rectifying K^+ current with biophysical, pharmacological, and regulation properties identical to the recently cloned TASK-1 and TASK-3 2P domain K^+ channels (30–35, 40, 41, 47–49). TASK-1 and TASK-3 are resistant to TEA and 4-AP, reversibly inhibited by extracellular acidosis and by activation of Gq-coupled receptors including the m3 receptor. The amplitude of IKso in cultured GN follows the temporal expression of TASK-1 and TASK-3 mRNAs, although TASK-3 seems to be the predominant player (see below).

Genetic Transfer of K^+ -dependent Cell Death to Hippocampal Neurons.—*In vitro* K^+ -dependent cell death is transferred to hippocampal neurons, lacking IKso, by expressing TASK-1 or TASK-3 channels. These TASK-expressing hippocampal neurons, similarly to the native GN, are protected by acidosis (pH 6.4) and by increasing extracellular K^+ . The lethal effect of TASK-3 is stronger and faster compared with TASK-1, but protection by extracellular pH and K^+ is weaker. The pK value of TASK-1 is in the range of the physiological pH (7.2–7.4), while a more acidic value (5.9–6.7) has been reported for TASK-3 (30–35, 40). The lower pH sensitivity of TASK-3 may thus explain the weaker protection observed at pH 6.4. When expressed in both hippocampal neurons and *Xenopus* oocytes, the amplitude of the TASK-3 current is substantially higher than that for TASK-1 (Ref. 46 and the present study). This important difference in expression level may be responsible for the weaker protection by high external K^+ (25 mM) on TASK-3-expressing hippocampal neurons. The induction of cell death requires TASK channel activity as the introduction of TASK-1 and TASK-3 loss of function mutants do not alter cell viability. It is interesting to note that TREK-1 WT does not induce cell death, while the constitutively active mutant E306A (54) mimics the effect of TASK channels. This further demonstrates that constitutive opening of the 2P domain K^+ channels induces death of cultured neurons. A previous report demonstrated that the kidney weak inward rectifier K^+ channel ROMK1, that is also open at rest, similarly induces hippocampal neuron apoptosis (7).

Protection of Granule Neurons by Genetic and Pharmacological Inactivation of Endogenous TASK Channels.—We used the dominant-negative loss of function mutants rTASK-1^{G95E} and rTASK-3^{G95E} to inactivate the endogenous TASK channels in cultured mature GN. Both rTASK-1^{G95E} and rTASK-3^{G95E} significantly reduce cell death of 8 DIV GN in culture. These results indicate that the activity of the TASK channels is prob-

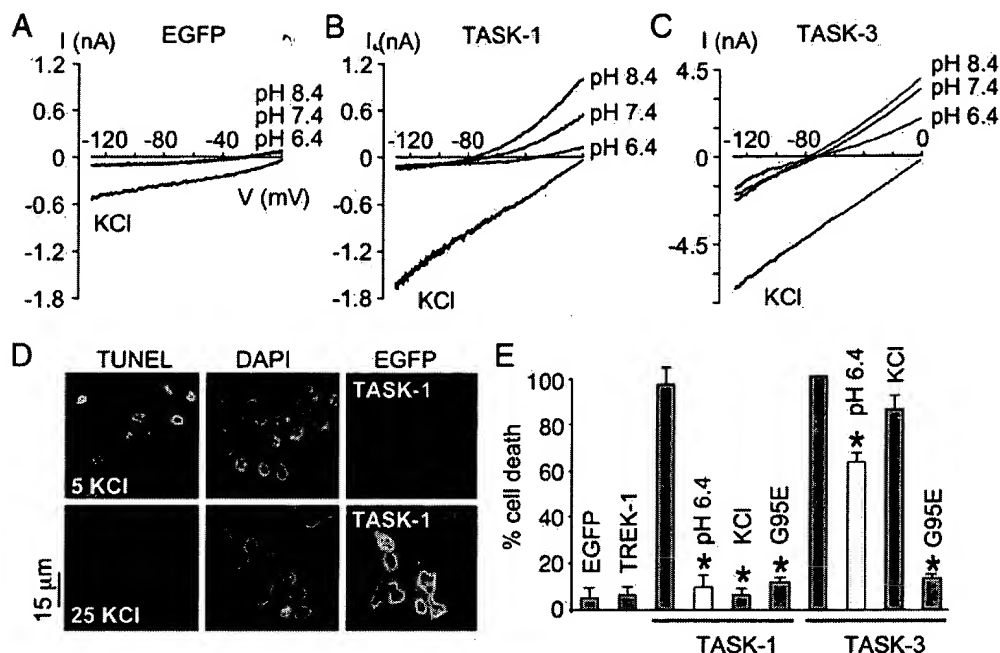


FIG. 7. Transfer of K^+ -dependent cell death by viral expression of TASK subunits in cultured rat hippocampal neurons. **A**, functional expression of EGFP in a SFV-infected hippocampal neuron (24 h). The neuron was held at a potential of 0 mV and voltage ramps of 500 ms in duration were applied every 10 s to -130 mV. Currents were recorded in the presence of 5 mM KCl at pH 8.4, 7.4, and 6.4 or in 125 mM KCl at pH 7.4. **B**, same as **A** with a hippocampal neuron expressing EGFP along with rTASK-1. **C**, same as **A** with a hippocampal neuron expressing EGFP along with rTASK-3. Note the different current scales in **B** and **C**. **D**, immunofluorescent images of TUNEL (red) and DAPI (blue) labeling, and EGFP fluorescence (green) in hippocampal neurons infected with TASK-1/EGFP incubated in either 5 mM K^+ (top) or 25 mM K^+ (bottom). **E**, quantitative analysis of hippocampal neuron viability at 24 h (TASK-1, EGFP, and TREK-1) and 16 h (TASK-3) postinfection. The histogram represents the number of dying EGFP positive neurons estimated by DAPI labeling. All data are from four independent experiments and reported as mean \pm S.E.

ably linked to the low K^+ -induced cell death of developing GN *in vitro*. The present report also supports the earlier evidence that TASK-1 and TASK-3 subunits may co-assemble to form a heteromultimeric channel at least when expressed in *Xenopus* oocytes (40). Dimeric TASK-1/TASK-3 channels, expressed independently or as tandem constructs, display intermediate pH sensitivity and intermediate inhibition by Gq-coupled receptor stimulation, thus demonstrating heteromultimeric assembly (40). Another recent study has however failed to demonstrate heteromultimerization between TASK-1, TASK-3, and TASK-5, an electrically silent subunit (46). Since TASK-1 and TASK-3 can form a heteromultimeric complex, the dominant-negative mutants do not allow discrimination between channel subunits. Four types of background K^+ channels related to TASK-1, TASK-3, TREK-2, and to an as yet unidentified channel have recently been described in rat-cultured GN (49). Taken together these results strongly suggest that the homomultimeric TASK-1, TASK-3, and possibly the heteromultimeric TASK-1/TASK-3 channels, are contributing to IK_{so} and thus may directly influence GN K^+ -dependent cell death in culture.

We have used a pharmacological approach to determine which of the TASK subunits is involved in GN cell death. Ruthenium red, a polycationic dye, blocks TASK-3 although it fails to affect TASK-1 and the heteromultimer TASK-1/TASK-3 (38, 52). By contrast, the endocannabinoid anandamide, at low concentrations, is a preferential blocker of TASK-1, independently of the CB receptors (37). Ruthenium red, unlike anandamide, fully blocks IK_{so} in the micromolar range and protects GN. These pharmacological results suggest that the homomultimer TASK-3 is dominant in GN K^+ -dependent death in culture. The pK value for TASK-3 is in the range of 5.9–6.7 (30, 32–34, 40) that corresponds to the value presently found for IK_{so} of 6.7. GN are half-protected from K^+ withdrawal at about

pH 7.0. The slight difference of 0.3 pH units between these pKs may reveal a non-linearity between IK_{so} , K^+ efflux and cell death, the eventual synergistic contribution of TASK-1 (pK_a of 7.2–7.4) or the involvement of another pH-sensitive mechanism such as the acid-inhibited type 4 baseline K^+ channel (49), the proton-gated cationic channels ASIC or TRPV that could also contribute to depolarize and thus protect neurons.

Intracellular K^+ and Neuronal Apoptosis—The link between K^+ channels, apoptosis, survival and proliferation has become increasingly recognized over the recent years (3–9, 11, 12, 55). For instance, apoptosis of mouse neocortical neurons induced by serum deprivation or by staurosporine is associated with an early enhancement of voltage-dependent delayed rectifier current and consequent loss of intracellular K^+ (5). Cortical neuron apoptosis is reversed by increasing extracellular K^+ or by pharmacological inhibition of the Kv channels. Interestingly, staurosporine- and serum starvation-induced GN apoptosis occur in both a K^+ -rich and an acidic culture medium. These results suggest that, a mechanism independent of K^+ channels, including TASK, is probably at play in this specific type of GN death, unlike the K^+ -dependent cell death *in vitro*. K^+ has previously been proposed to contribute to the apoptotic phenotype by two distinct, but not necessarily independent, mechanisms. First, K^+ efflux is associated with an osmolytic water loss leading to apoptotic volume decrease (AVD), a key initial apoptotic event (56, 57). Second, K^+ has been suggested to be an important negative regulator of intracellular enzymes, such as nucleases and caspases, which play a strategic role in apoptosis (56, 57).

The present study indicates that, in culture, there is a good correlation between TASK/ IK_{so} amplitude and rat GN K^+ -dependent death. However, the interpretation of this data needs to take into account that multiple other molecular pathways are also involved in the control of GN cell survival/death. Fur-

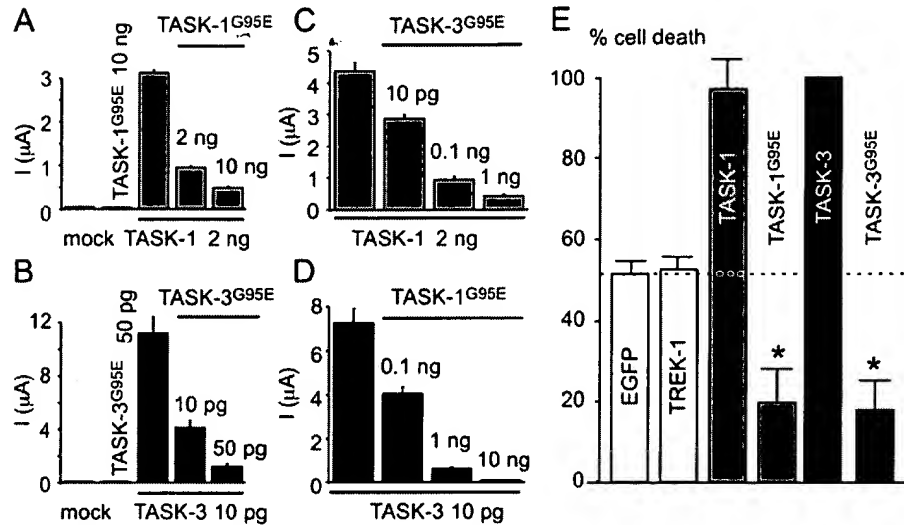


FIG. 8. Protection of cultured rat cerebellar granule neurons by expression of rTASK-3^{G95E} and rTASK-1^{G95E} dominant-negative mutants. A, earlier studies have reported that the G95E mutation in the first selectivity filter of 2P domain K⁺ channels induces a loss of function (46). In agreement with this report, electrophysiological recordings in *Xenopus* oocytes demonstrate that TASK-1^{G95E} behaves as a dominant-negative against WT TASK-1. In the experiments illustrated in this figure, the amount of mRNA injected was constant and adjusted with the mRNA encoding FaNaC, a ligand-gated sodium channel silent in the absence of FRMFamide. The amount of TASK or mutant mRNA injected per oocyte is indicated. The mRNAs were *in vitro* transcribed from a pEXO vector containing the 5'- and 3'-untranslated region of *Xenopus* globin. Currents were recorded with voltage ramps of 800 ms in duration from -120 mV to 100 mV applied every 10 s from a holding potential of -80 mV. Currents were measured at 0 mV. Each data point is the mean of 20 oocytes. B, same procedure with TASK-3^{G95E}. Note that in these experiments TASK-3 mRNA was diluted by 200-fold compared with TASK-1 illustrated in A. Each data point is the mean of 10–15 oocytes. The loss of function TREK-1^{G144E} mutant did not affect TASK-1 ($n = 28$) or TASK-3 ($n = 27$) currents even with a 100-fold mRNA excess (not shown). C, heteromultimeric association between TASK-1 and TASK-3 has been previously proposed (52). Present experiments using TASK^{G95E} loss of function mutants support this earlier statement. TASK-3^{G95E} behaves as a dominant-negative mutant when co-expressed with TASK-1 WT. The dominant-negative effect is dose-dependent. Each data point is the mean of 15 oocytes. D, TASK-1^{G95E} behaves as a dominant-negative mutant when co-expressed with TASK-3 WT. The dominant-negative effect is dose-dependent. Each data point is the mean of 12–19 oocytes. E, quantitative analysis of GN viability after 6 h incubation in the low K⁺ condition containing 5 mM KCl. The histogram represents % of apoptotic EGFP expressing GN estimated by DAPI staining. The dashed line indicates the level of apoptotic cell death in EGFP-infected GN. All data are from four independent experiments and reported as mean \pm S.E. In these *Xenopus* oocyte and GN experiments, all rat TASK channels were tagged at the amino terminus with hemagglutinin.

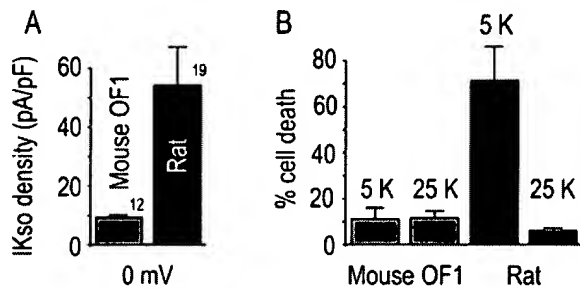


FIG. 9. OF1-cultured cerebellar granule neurons are resistant to K⁺ withdrawal. A, the current density of IKso is significantly smaller in murine OF1 GN compared with rat GN cultured under identical conditions (8–9 DIV). Currents were recorded with voltage ramps of 800 ms in duration from -120 mV to 100 mV applied every 10 s from a holding potential of -80 mV. Currents were measured at 0 mV in the external medium containing 5 mM K⁺ at pH 7.4. B, murine OF1, unlike rat GN survives in the 5 K⁺ condition. GN were cultured for 8–9 days under the 25 K⁺ condition and was subsequently shifted to the low K⁺ condition for 8 h and analyzed for cell viability by PI labeling.

thermore, the limitation of the experimental procedures that have been used should be carefully considered. For instance, besides TASK channels, lowering extracellular pH will clearly affect other types of ion channels including VR1, ASIC and NMDA, and also induce a large number of effects unrelated to ion channels within the cells. Similarly, at the pharmacological level, ruthenium red, which preferentially blocks TASK-3 and protects GN from cell death, may also affect multiple other important targets including other 2P domain K⁺ channels such as TRAAK or the ryanodine receptor among others (38).

Our data confirm that overexpression of a K⁺-selective chan-

nel, which is open at rest, can lead to cell death *in vitro* as seen with rat hippocampal neurons (7). Protection of rat GN by expression of TASK^{G95E} dominant-negative mutants, indicates that TASK background K⁺ channels may similarly contribute significantly to the K⁺-dependent rat GN cell death in culture. The correlation between the reduced IKso amplitude and the ability of cultured murine OF1 GN to survive in low K⁺ conditions, further suggests a close relationship between TASK/IKso current amplitude and K⁺-dependent cell death. It is interesting to note that GN from the C57BL/6 mouse strain express a large IKso (47) and undergo apoptosis *in vitro*, similarly to rat neurons, in a physiological K⁺ medium (58).² A key question remains as to whether there is a similar relationship between TASK channel activity and developmental GN apoptosis *in vivo*. The increase in the levels of TASK-3 (about 6-fold) and to a lesser extent TASK-1 (about 3-fold) transcripts in culture complicates the comparison between the *in vitro* and *in vivo* situations. The knock out of TASK subunits will certainly be valuable to directly assay the role of these channels during *in vivo* GN developmental apoptosis. However, the absence of a significant IKso in the murine OF1 GN suggests that alternative or parallel mechanisms are also at play during development.

While this article was submitted, an interesting report has appeared demonstrating the genomic amplification and the oncogenic properties of KCNK9 (TASK-3) (12). TASK-3 transcript is overexpressed from 5-fold to over 100-fold in 44% of breast tumors. Overexpression of TASK-3 in cell lines promotes

² A. J. Patel, I. Lauritzen, E. Honoré, M. Lazdunski, unpublished data.

tumor formation and confers resistance to both hypoxia and serum deprivation, suggesting that its amplification and overexpression plays a direct role in human breast cancer (12). TASK-1 and TASK-3 channels are reversibly inhibited by hypoxia and have previously been implicated in the chemoreception of both type I carotid body cells and lung neuroepithelial body cells (45, 59). It has been speculated that the oncogenic effect of TASK-3 may be related to its ability to respond to oxygen (12). This is particularly relevant to cancer pathology because of the poorly oxygenated areas of solid tumors (12). These results, further suggest an important role for the TASK channel subunits in the control of cell proliferation/cell death. Dysregulation of TASK transcription/translation/turnover that might occur in disease states and possibly during aging may thus have important functional implications for both cellular excitability and survival (12, 47). The recently discovered TASK molecular partners (p11 and 14-3-3) that regulate channel trafficking could also influence cell survival by modulating TASK-1/3 channel expression (60–62).

TASK channels are opened by volatile general anesthetics including halothane and isoflurane (26, 44). Early exposure to inhalational anesthetics, causes widespread neurodegeneration in the developing brain with persistent impairments and represents a potential problem in pediatric and obstetric anesthesia (63). The stimulation of TASK opening should therefore be considered in volatile anesthetics-induced neurodegeneration. The development of specific modulators of TASK-1/3 channels may be a useful pharmacological strategy for the treatment of neurodegenerative and/or proliferative diseases.

Acknowledgments—We thank Dr. F. Lesage for critical comments on the article. We thank Dr. C. Alves Da Costa for appreciated help with caspase activity measurements. We thank Drs. Kenneth Lundstrom and Sondra Schlesinger for helpful comments on the generation of pSFV(PD)-Sub-GFP. Valérie Briet is acknowledged for expert assistance with the manuscript. Martine Jodar and Valérie Friend are acknowledged for excellent technical assistance. Morgane Rouault is acknowledged for advice on real-time PCR. We thank Dr. Spencer Yost for the generous gift of rTASK-1 cDNA and Dr. Vincenzo Di Marzo for the gift of VDM11.

REFERENCES

- Pettmann, B., and Henderson, C. E. (1998) *Neuron* **20**, 633–647
- Yuan, J., and Yankner, B. A. (2000) *Nature* **407**, 802–808
- Maeno, E., Ishizaki, Y., Kanaseki, T., Hazama, A., and Okada, Y. (2000) *Proc. Natl. Acad. Sci. U. S. A.* **97**, 9487–9492
- Hughes, F. M. J., Bortner, C. D., Purdy, G. D., and Cidlowski, J. A. (1997) *J. Biol. Chem.* **272**, 30567–30576
- Yu, S. P., Yeh, C. H., Sensi, S. L., Gwag, B. J., Canzoniero, L. M., Farhangrazi, Z. S., Ying, H. S., Tian, M., Dugan, L. L., and Choi, D. W. (1997) *Science* **278**, 114–117
- Yu, S. P., Yeh, C., Strasser, U., Tian, M., and Choi, D. W. (1999) *Science* **284**, 336–339
- Nadeau, H., McKinney, S., Anderson, D. J., and Lester, H. A. (2000) *J. Neurophysiol.* **84**, 1062–1075
- Heurteaux, C., Bertina, V., Widmann, C., and Lazdunski, M. (1993) *Proc. Natl. Acad. Sci. U. S. A.* **90**, 9431–9435
- Lauritzen, I., De Wille, J. R., and Lazdunski, M. (1997) *J. Neurochem.* **69**, 1570–1579
- Yuan, A., Santi, C. M., Wei, A., Wang, Z.-W., Pollak, K., Nonet, M., Kaczmarek, L., Crowder, M., and Salkoff, L. (2003) *Neuron* **37**, 765–773
- Pardo, L. A., del Camino, D., Sanchez, A., Alves, F., Bruggemann, A., Beckh, S., and Stühmer, W. (1999) *EMBO J.* **18**, 5540–5547
- Mu, D., Chen, L., Zhang, X., See, L.-H., Koch, C. M., Yen, C., Tong, J. J., Spiegel, L., Nguyen, K. C. Q., Servoss, A., Peng, Y., Pei, L., Marks, J. R., Lowe, S., Hoey, T., Jan, L. Y., McCombie, W. R., Wigler, M. H., and Powers, S. (2003) *Cancer Cell* **3**, 297–302
- Smith, G. A., Tsui, H. W., Newell, E. W., Jiang, X., Zhu, X. P., Tsui, F. W., and Schlichter, L. C. (2002) *J. Biol. Chem.* **277**, 18528–18534
- Wang, H., Zhang, Y., Cao, L., Han, H., Wang, J., Yang, B., Nattel, S., and Wang, Z. (2002) *Cancer Res.* **62**, 4843–4848
- Lossi, L., Mioletti, S., and Merighi, A. (2002) *Neuroscience* **112**, 509–523
- Gallo, V., Kingsbury, A., Balazs, R., and Joergensen, O. S. (1987) *J. Neurosci.* **7**, 2203–2213
- Wood, K. A., Dipasquale, B., and Youle, R. J. (1993) *Neuron* **11**, 621–632
- Yan, G.-M., Ni, B., Weller, M., Wood, K. A., and Paul, S. M. (1994) *Brain Res.* **656**, 43–51
- Galli, C., Meucci, O., Scorziello, A., Werge, T. M., Calissano, P., and Schettini, G. (1995) *J. Neurosci.* **15**, 1172–1179
- Mao, Z., Bonni, A., Xia, F., Nadal-Vicens, M., and Greenberg, M. E. (1999) *Science* **286**, 785–790
- Bennett, M., and White, W. (1981) *Brain Res.* **173**, 549–553
- Chalazonitis, A., and Fishbach, G. D. (1980) *Dev. Biol.* **78**, 173–183
- Phillipson, D. T., and Sandler, M. (1975) *Brain Res.* **90**, 273–281
- Scott, B. S. (1977) *J. Cell. Physiol.* **91**, 305–316
- Lesage, F., and Lazdunski, M. (2000) *Am. J. Physiol. Renal Physiol.* **279**, F793–801
- Patel, A. J., and Honoré, E. (2001) *Trends Neurosci.* **2**, 422–426
- Bayliss, D. A., Talley, E. M., Sirois, J. E., and Lei, Q. (2001) *Respir. Physiol.* **129**, 159–174
- Goldstein, S. A. N., Bockenhauer, D., O'Kelly, I., and Zilberberg, N. (2001) *Nat. Rev. Neurosci.* **2**, 175–184
- Lesage, F., Reyes, R., Fink, M., Duprat, F., Guillemare, E., and Lazdunski, M. (1996) *EMBO J.* **15**, 6400–6407
- Lopes, C. M., Zilberberg, N., and Goldstein, S. A. (2001) *J. Biol. Chem.* **276**, 24449–24452
- Duprat, F., Lesage, F., Fink, M., Reyes, R., Heurteaux, C., and Lazdunski, M. (1997) *EMBO J.* **16**, 5464–5471
- Kim, Y., Bang, H., and Kim, D. (2000) *J. Biol. Chem.* **275**, 9340–9347
- Meadows, H. J., and Randall, A. D. (2001) *Neuropharmacology* **40**, 551–559
- Rajan, S., Wischmeyer, E., Liu, G. X., Preisig-Müller, R., Daut, J., Karschin, A., and Derst, C. (2000) *J. Biol. Chem.* **275**, 16650–16657
- Kim, D., Fujita, A., Horio, Y., and Kurachi, Y. (1998) *Circ. Res.* **82**, 513–518
- Leonoudakis, D., Gray, A. T., Winegar, B. D., Kindler, C. H., Harada, M., Taylor, D. M., Chavez, R. A., Forsayeth, J. R., and Yost, C. S. (1998) *J. Neurosci.* **18**, 868–877
- Maingret, F., Patel, A. J., Lazdunski, M., and Honoré, E. (2001) *EMBO J.* **20**, 47–54
- Czirjak, G., and Enyedi, P. (2003) *Mol. Pharmacol.* **63**, 646–652
- Talley, E. M., Lei, Q., Sirois, J. E., and Bayliss, D. A. (2000) *Neuron* **25**, 399–410
- Czirjak, G., Petheo, G. L., Spat, A., and Enyedi, P. (2001) *Am. J. Physiol. Cell Physiol.* **281**, C700–708
- Millar, J. A., Barratt, L., Southan, A. P., Page, K. M., Fyffe, R. E. W., Robertson, B., and Mathie, A. (2000) *Proc. Natl. Acad. Sci. U. S. A.* **97**, 3614–3618
- Plant, L. D., Kemp, P. J., Peers, C., Henderson, Z., and Pearson, H. A. (2002) *Stroke* **33**, 2324–2328
- Barbuti, A., Ishii, S., Shimizu, T., Robinson, R. B., and Feinmark, S. J. (2002) *Am. J. Physiol. Heart Circ. Physiol.* **282**, H2024–H2030
- Patel, A. J., Honoré, E., Lesage, F., Fink, M., Romey, G., and Lazdunski, M. (1999) *Nat. Neurosci.* **2**, 422–426
- Buckler, K., Williams, B., and Honoré, E. (2000) *J. Physiol.* **525**, 135–142
- Karschin, C., Wischmeyer, E., Preisig-Müller, R., Rajan, S., Derst, C., Grzeschik, K. H., Daut, J., and Karschin, A. (2001) *Mol. Cell Neurosci.* **18**, 632–648
- Brickley, S. G., Revilla, V., Cull-Candy, S. G., Wisden, W., and Farrant, M. (2001) *Nature* **409**, 88–92
- Watkins, C. S., and Mathie, A. (1996) *J. Physiol.* **492**, 401–412
- Han, J., Truell, J., Gnatenco, C., and Kim, D. (2002) *J. Physiol.* **542**, 431–444
- Eldadah, B. A., Yakolev, A. G., and Faden, A. I. (1997) *J. Neurosci.* **17**, 6105–6113
- Daniels, M., and Brown, D. R. (2002) *Mol. Cell Neurosci.* **19**, 281–291
- Czirjak, G., and Enyedi, P. (2002) *J. Biol. Chem.* **277**, 5426–5432
- Lundström, K., Rotmann, D., Hermann, D., Schneider, E. M., and Ehrengruber, M. U. (2001) *Histochem. Cell Biol.* **115**, 83–91
- Honoré, E., Maingret, F., Lazdunski, M., and Patel, A. J. (2002) *EMBO J.* **21**, 2968–2976
- Trimarchi, J. R., Liu, L., Smith, P. J. S., and Keefe, D. L. (2002) *Am. J. Physiol. Cell Physiol.* **282**, C588–C594
- Yu, S. P., and Choi, D. W. (2000) *Proc. Natl. Acad. Sci. U. S. A.* **97**, 9360–9362
- Okada, Y., Maeno, E., Shimizu, T., Dezaki, K., Wang, J., and Morishima, S. (2001) *J. Physiol.* **532**, 3–16
- Fujikawa, N., Tominaga-Yoshino, K., Okabe, M., and Ogura, A. (2000) *Eur. J. Neurosci.* **12**, 1838–1842
- Hartness, M. E., Lewis, A., Searle, G. J., O'Kelly, I., Peers, C., and Kemp, P. J. (2001) *J. Biol. Chem.* **276**, 26499–26508
- Girard, C., Tinel, N., Terrenoire, C., Romey, G., Lazdunski, M., and Borsotto, M. (2002) *EMBO J.* **21**, 4439–4448
- Rajan, S., Preisig-Müller, R., Wischmeyer, E., Nehring, R., Hanley, P. J., Renigunta, V., Musset, B., Schlichthorl, G., Derst, C., Karschin, A., and Daut, J. (2002) *J. Physiol.* **545**, 13–26
- O'Kelly, I., Butler, M., Zilberberg, N., and Goldstein, S. (2002) *Cell* **111**, 577–588
- Jevtic-Todorovic, V., Hartman, R. E., Izumi, Y., Benshoff, N. D., Dikranian, K., Zorumski, C. F., Olney, J. W., and Wozniak, D. F. (2003) *J. Neurosci.* **23**, 876–882